Advances in Continuous and Discrete Models

RESEARCH Open Access

Dynamic analysis of SPAFIR epidemic model considering pseudoinfection and perturbations

Xiaoqian Nie[1], Yuhan Hu[1*] and Weijun Yan[2]

*Correspondence:
anshanhyh@163.com
[1]School of Science, University of Science and Technology Liaoning, Qianshan Middle Road, Anshan, 114051, Liaoning, China
Full list of author information is available at the end of the article

Abstract

In this paper, the "pseudoinfection phenomenon" and "individual behavioral responses" are taken into account in the SIR epidemic model, and the deterministic and stochastic models are analyzed dynamically. Through the exploration of the deterministic SPAFIR (Susceptible-Pseudoinfected-Alert-Fragile-Infected-Recovered) model, the conditions for the equilibrium points' existence and stability are determined. With the assistance of the Pontryagin maximum principle, this paper introduces a Hamiltonian function with a penalty term and the optimal control strategy is obtained by comparing the three groups of strategies. The optimal control strategy requires multiple control measures to inhibit the infectious disease spread. Further considering the stochastic SPAFIR model, the existence of the uniqueness of a global positive solution and the existence of a stationary distribution for the stochastic model are proved, and the condition for disease extinction is also verified. Random perturbations of the effective contact rates can slow the pace of spreading the infectious diseases. Results of theoretical analysis and the system's responsiveness to variations in effective contact rates are verified by numerical simulations, and the outcomes indicate that active prevention education and community encouragement can both inhibit infection spread.

Keywords: SPAFIR epidemic model; Pseudoinfection; Differential equation; Stability analysis; Random perturbations

1 Introduction

In history, the massive spread of infectious diseases had brought great disasters and had a huge impact on society [1–3]. For instance, in medieval Europe, the plague caused over 50 percent of the population to die in different regions of the continent. The massive outbreak of cholera caused social instability in nineteenth-century England and Ireland, and AIDS broke out globally in the late twentieth century, resulting in serious population fatalities and economic impacts. The rapid development of medical devices and technologies, alongside the improvement of living and economic conditions, has reduced the threat of infectious diseases to human health. This has led to decreased morbidity and mortality rates, and effective control of many infectious diseases. However, with the further acceleration of globalization and urbanization, and the changes in human lifestyles, the transmis-

sion speed and range of infectious diseases may be faster than ever before, and the issue of infectious diseases is still a concern, especially the emergence and spread of emerging viruses [4, 5], such as those that have reduced economic output [6, 7] and caused severe declines in the tourism industry [8–10]. Given that epidemics have affected businesses in various countries and regions, studying the mechanisms by which infectious diseases are transmitted has become crucial.

Epidemic models have been used for more than two hundred years to help understand how infectious diseases spread. This dates back to 1760, when Bernoulli [11] carried out a mathematical analysis of smallpox. He proposed the theory of vaccination as a means of preventing the disease. In 1927, Kermack and McKendrick [12] simulated the transmission process of different infectious diseases using differential equations and established the classical SIR model, which provided an important theoretical basis for the study of epidemic dynamics models. In 1957, Bailey [13] used mathematical tools such as differential equations and stochastic processes to theoretically describe an infectious disease and its outbreak mechanism. In 2000, Hethcote [14] reviewed epidemic dynamics and introduced major mathematical models, as well as quantitative methods for modeling and predicting outbreaks and transmission of infectious diseases. In the last 30 years, a multitude of mathematical models have been created by scholars to depict various transmission attributes of infectious diseases, such as models with nonlinear incidence rates [15–18], models with bilinear linear incidence rates [19–21], models characterized by network structures [22–24], and models characterized by spatial diffusion [25–27]. These models are extremely versatile theoretical tools that provide us with indispensable help in gaining a deeper understanding of the dynamic progress of disease spread and in assessing the validity for epidemiological defence and control measures.

By analyzing epidemiological transmission mechanisms, it has been possible to gain some insight into infection characteristics and transmission routes. Some researchers have explored new approaches to infectious-disease spread by transforming some parameters into time-dependent control variables. Zaman et al. [28] provided an indepth discussion on the propagation of the SIR model in regular and small-world networks. Based on the known infectious disease parameters, they employed optimal control theory to determine the optimal vaccination strategy. It was suggested that targeted vaccination and network topology-based vaccination strategies were more efficient than random vaccination in controlling and reducing infection spread. By varying parameters such as susceptible rate, infected rate, and exposure rate, Zhang et al. [29] developed a saturated exposure-rate SEIR prevalence model, and proposed control measures to respond to epidemic emergence and transmission, such as raising health awareness and enhancing medical safety to curb disease spread. To describe the time delay of infection, Laarabi et al. [30] used the theory of delay dynamics, established an ODE mathematical model with control delay based on two control strategies, vaccination and treatment, and proposed appropriate vaccination and therapeutic measures for the control and eradication of the disease.

The epidemic models mentioned above are largely deterministic models that have almost no consideration of the impact of stochastic factors in the natural environment on disease transmission. In fact, stochastic factors in the natural environment are ubiquitous and have an impact on population dynamic behavior [31]. In the past decade, more and more scholars have explored the impact of stochastic factors on the mechanisms of disease transmission. Tornatore et al. [32] established a stochastic SIR model using stochastic dif-

ferential equations, studied the impact of stochastic factors on the SIR model, determined the conditions for system stability through mathematical analysis and numerical simulations, and investigated the effects of stochastic disturbances on the model and its corresponding prevention and control strategy. Wei et al. [33] developed a stochastic model of SIQS in which there is an incidence of saturation and in which this incidence is affected by independent random disturbances. For epidemic models that include stochastic factors, investigating the threshold conditions for extinction is of great theoretical significance and practical value. Gray et al. [34] investigated a stochastic SIS model to analyze the 2019-nCoV pandemic transmission dynamics using a fractal fraction operator, creating appropriate conditions for disease eradication and persistence. To describe the stochasticity of the number of superspreaders and implicitly exposed individuals, Kang et al. [35]used a stochastic differential-equation approach, and explored the impact of randomness on the propagation model through theoretical analysis of a probability model and stochastic processes. This provided a theoretical basis for establishing optimal control strategy, and the same stochastic factors can also be applied to the same epidemic propagation model.

In epidemic models, changes in individual behavior can result in different epidemic model outcomes. Fenichel et al. [36] revealed that human individual behavioral responses can significantly affect the results of epidemic models, and proposed that these response factors should be incorporated into epidemiological models to more accurately predict the spread and outbreak of diseases. Sahneh et al. [37] found that individual behavioral responses are one of the important factors influencing how infectious diseases spread. Epidemiological models that consider human individual behavioral responses show significant effects, and can greatly reduce the risk of virus transmission. In some cases, forced isolation or restrictions on people's activities may have the opposite effect, and encouraging and improving individual behavior in response to interventions can reduce the likelihood of infection and spread.

This paper considers the combination of "pseudoinfection" and "individual behavioral responses" on the basis of the classical SIR model. "Pseudoinfection" refers to the same symptoms as virus infection but without being infected and contagious, such as the outbreak of COVID-19, whose symptoms include cold, fever, cough, runny nose, etc. Pseudoinfected individuals have these symptoms, but they are not infected with the COVID-19 virus and are not contagious. At the same time, the behavioral responses of pseudoinfected individuals can be divided into three categories: i) Actively responding to their own "infection" and remaining vigilant. ii) Passively responding to their own "infection" and remaining vulnerable. iii) Responding to their own "infection" with a calm mindset and taking no action, in which case the pseudoinfected individuals can be regarded as susceptible individuals. This paper constructs a deterministic model considering the phenomena of "pseudoinfection" and "individual behavioral response", and examines the effect of pseudoinfected individuals' behavior on disease spread using a control strategy. In addition, the impact on disease transmission when the effective contact rate is affected by random perturbations is considered, and the condition under which the disease elimination threshold is reached is explored.

The remaining sections are then structured in the following way. In Sect. 2, taking into account the phenomena for "pseudoinfection" and "individual behavioral responses", a deterministic SPAFIR model is constructed. In Sect. 3, after calculating R_0, local and global asymptotic stability for equilibrium points are proved. Section 4 presents a control strategy

for limiting infection spread. Section 5 establishes a stochastic SPAFIR model with effective contact rates subject to stochastic disturbances. In Sect. 6, a global positive solution exists in the stochastic model, which is shown to be unique. In addition, the condition for the elimination of disease is provided. Validated by numerical simulations, Sect. 7 further confirms the stability of the equilibrium points and analyzes the efficacy for optimal control strategy, as well as the condition for achieving disease elimination under the stochastic model. Section 8 analyzes the sensitivity of infectious disease transmission to changing effective contact rates. The last section consists of conclusions and future prospects.

2 The deterministic model

During an outbreak caused by a specific strain of a virus, with fluctuations in time t, the population size $\mathcal{N}(t)$ changes. In order to describe their characteristics and behavior, the population size can be grouped according to six different categories: (1) The susceptible group includes those who risk becoming infected but are not currently infected, is denoted by $S(t)$. (2) The pseudoinfected class is represented by $P(t)$, refers to individuals who exhibit symptoms identical to those of a viral infection but are neither infected nor contagious. These symptoms, influenced by external environmental factors or reduced immune function, are clinically consistent with those of actual infected individuals. However, these individuals do not carry the virus, and their symptoms are not caused by a viral infection. (3) The alert class, denoted as $A(t)$, refers to individuals who exhibit symptoms similar to those of a viral infection but are noncontagious. These symptoms may partially overlap with typical manifestations of viral infections; however, they are not caused by actual infection but may result from environmental factors or reduced immune function. Triggered by subjective cognition and psychological responses, these individuals subconsciously perceive themselves as being infected and adopt proactive measures to address this "perceived infection", such as seeking medical assistance, self-isolating, or taking steps to improve their health condition. (4) The fragile class, represented as $F(t)$, also refers to individuals who exhibit symptoms resembling those of a viral infection but are noncontagious. Driven by psychological and cognitive factors, these individuals subconsciously believe they are infected. However, unlike those in the $A(t)$ category, they typically respond to this "perceived infection" in a negative manner, such as displaying anxiety, fear, or psychological withdrawal. (5) $I(t)$ represents the infected class, which consists of infected and contagious individuals. (6) $R(t)$ denotes the recovery class, which consists of immune individuals who are not infected with the disease.

In the constructed model, a pseudoinfected state is introduced after the susceptible state. The behavioral responses of the pseudoinfected individuals have the following manifestations: If the pseudoinfected individuals actively deal with the "infection" that the individuals themselves think they have, their psychology is positive and optimistic, and then they enter the alert state. If the pseudoinfected individual responds passively to the "infection", the psychological depression is heavy and the pseudoinfected individuals enter the fragile state from the pseudoinfected state. If the pseudoinfected individuals treat their "infection" calmly, they return to the susceptible state. Considering individual behavioral responses, susceptible individuals, alert individuals, and fragile individuals have different effective contact rates when contacting with infected individuals. This paper establishes a deterministic SPAFIR model considering a "pseudoinfection phenomenon" and "individual behavioral responses". Figure 1 presents the SPAFIR epidemic state-transition diagram, which is used to describe the transition process between different states.

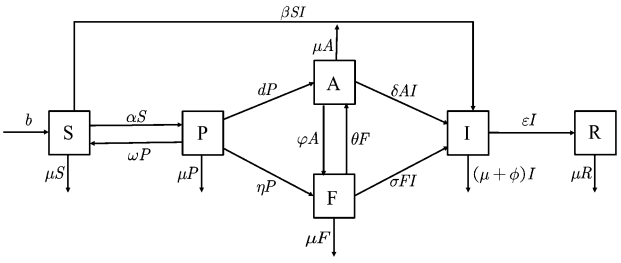

Figure 1 State transition diagram for the SPAFIR epidemic model

Parameters are defined to provide a clearer understanding of their meaning and role in the SPAFIR epidemic model. Each parameter has a specific role and function in the model, the meanings of the parameters are as follows:

- The fluctuation in the population of a system over time is considered. To describe this phenomenon more clearly, the parameter b is described as the number of immigrants. However, some individuals may leave the system due to unforeseeable circumstances, such as natural death, so this paper uses μ to define the natural removal rate. In addition, the infectious mortality rate ϕ of infected individuals due to the infectious disease is also considered in this paper.
- When the virus begins to spread in the system, a portion of the susceptible individuals become infected by contact with infected individuals, and the effective contact rate is denoted by β. There are also some susceptible individuals who may directly enter a pseudoinfection state at a proportion of α, influenced by external environmental factors or reduced immune function, without requiring contact with infected individuals. This mechanism is based on the impact of noninfectious factors on individual health, including environmental pressure, and physiological changes. Meanwhile, pseudoinfected individuals treat their "infection" calmly and transform into susceptible individuals with a probability of ω.
- When pseudoinfected individuals actively face their "infection", this group will transform into alert individuals at a proportion of d. Similarly, when pseudoinfected individuals passively face their "infection", they transform into fragile individuals at a probability of η. Simultaneously, both alert and fragile individuals can transform into each other due to external interference. For example, alert individuals may be rejected and isolated by others due to the possibility of infection, causing their reactions to become passive, leading to a transformation into fragile individuals at a rate of φ. Fragile individuals may enter an alert state at a probability of θ due to external stimulation, and this process is closely related to the external environment.
- When there are infected individuals, alert and fragile individuals have some probability of contacting them and becoming infected, and the effective contact rates of alert and fragile individuals are specified as δ and σ, respectively. For alert individuals, positive individual responses can effectively enhance immune capacity, thereby increasing resistance to pathogens. This immunity-boosting effect significantly reduces the likelihood of alert individuals becoming infected. In contrast, for fragile individuals, negative individual responses may lead to further weakening of the immune system, increasing the risk of infection. Therefore, it is reasonable to

assume that $\delta < \sigma$ holds. Meanwhile, infected individuals are cured and enter the recovery state at a rate of ε, where they acquire immunity.

From the above analysis, the system dynamics equations are as shown below:

$$\begin{cases} \frac{dS}{dt} = b - \alpha S - \beta SI - \mu S + \omega P, \\ \frac{dP}{dt} = \alpha S - \omega P - dP - \eta P - \mu P, \\ \frac{dA}{dt} = dP - \delta AI + \theta F - \varphi A - \mu A, \\ \frac{dF}{dt} = \eta P - \sigma FI + \varphi A - \theta F - \mu F, \\ \frac{dI}{dt} = \delta AI + \sigma FI + \beta SI - \varepsilon I - (\mu + \phi)I, \\ \frac{dR}{dt} = \varepsilon I - \mu R. \end{cases} \tag{1}$$

By merging the coefficients of the similar terms in system (1), system (2) can be obtained, and both system (1) and system (2) can represent the same system. For the sake of discussion, this paper will only consider system (2):

$$\begin{cases} \frac{dS}{dt} = b - m_1 S - \beta SI + \omega P, \\ \frac{dP}{dt} = \alpha S - m_2 P, \\ \frac{dA}{dt} = dP - \delta AI + \theta F - m_3 A, \\ \frac{dF}{dt} = \eta P - \sigma FI + \varphi A - m_4 F, \\ \frac{dI}{dt} = \delta AI + \sigma FI + \beta SI - m_5 I, \\ \frac{dR}{dt} = \varepsilon I - \mu R, \end{cases} \tag{2}$$

where

$$\begin{aligned} &b, \alpha, d, \eta, \theta, \varphi, \beta, \delta, \sigma, \omega, \varepsilon, \phi, \mu > 0, \delta < \sigma, \\ &m_1 = \alpha + \mu, m_2 = \omega + d + \eta + \mu, m_3 = \varphi + \mu, \\ &m_4 = \theta + \mu, m_5 = \varepsilon + \mu + \phi \end{aligned} \tag{3}$$

and

$$\begin{aligned} &S(0) = S^0 \geq 0, A(0) = A^0 \geq 0, F(0) = F^0 \geq 0, \\ &P(0) = P^0 \geq 0, I(0) = I^0 \geq 0, R(0) = R^0 \geq 0, \end{aligned} \tag{4}$$

$$\mathcal{N}(t) = S(t) + A(t) + F(t) + P(t) + I(t) + R(t). \tag{5}$$

3 Deterministic model analysis

Lemma 1 *For $t \geq 0$, the closed set $\Pi^+ = \{(S(t), P(t), A(t), F(t), I(t), R(t)) \in R_+^6 : S \geq 0, P \geq 0, A \geq 0, F \geq 0, I \geq 0, R \geq 0, S(t) + P(t) + A(t) + F(t) + I(t) + R(t) \leq \frac{b}{\mu}\}$ is the positive invariant set of the model (2).*

Proof It is evident that $\frac{d\mathcal{N}}{dt} = b - \mu\mathcal{N} - \phi I \leq b - \mu\mathcal{N}$, so there exists $\frac{b}{\mu} - e^{-\mu t}(\frac{b}{\mu} - \mathcal{N}^0) \geq \mathcal{N}(t)$, in which $\mathcal{N}^0 = \mathcal{N}(0)$. There can be no doubt that $\lim_{t\to\infty} \mathcal{N}(t) \leq \frac{b}{\mu}$. Thus, for $t \geq 0$, the

positive invariant set for the model (2) is represented by:

$$\begin{aligned}\Pi^{+} =& \Big\{ \big(S(t), P(t), A(t), F(t), I(t), R(t)\big) \in R_{+}^{6} : S \geq 0, P \geq 0, A \geq 0, \\ & F \geq 0, I \geq 0, R \geq 0, S(t) + P(t) + A(t) + F(t) + I(t) + R(t) \leq \frac{b}{\mu} \Big\}.\end{aligned} \tag{6}$$

□

3.1 The basic reproduction number R_0

R_0 represents the next-generation number generated by a single virus spreader. Before calculating R_0, it is essential to determine the disease-free equilibrium point E_0. The equilibrium point $E = (S, P, A, F, I, R)$ can be computed from the kinetic equations (2). E must satisfy the following equations:

$$\begin{cases} b - m_1 S - \beta SI + \omega P = 0, \\ \alpha S - m_2 P = 0, \\ dP - \delta AI + \theta F - m_3 A = 0, \\ \eta P - \sigma FI + \varphi A - m_4 F = 0, \\ \delta AI + \sigma FI + \beta SI - m_5 I = 0, \\ \varepsilon I - \mu R = 0. \end{cases} \tag{7}$$

Let $I = 0$, then the disease-free equilibrium point $E_0 = (S_1, P_1, A_1, F_1, I_1, R_1)$ can be calculated easily and invariably exists, where:

$$\begin{aligned} & S_1 = \frac{bm_2}{m_1 m_2 - \omega\alpha}, P_1 = \frac{\alpha b}{m_1 m_2 - \omega\alpha}, A_1 = \frac{\alpha b(dm_4 + \theta\eta)}{(m_3 m_4 - \theta\varphi)(m_1 m_2 - \omega\alpha)}, \\ & F_1 = \frac{\alpha b(d\varphi + \eta m_3)}{(m_3 m_4 - \theta\varphi)(m_1 m_2 - \omega\alpha)}, I_1 = 0, R_1 = 0. \end{aligned} \tag{8}$$

Let $X = (I, A, F, S, P, R)$, then model (2) can be written as $\frac{dX}{dt} = \mathcal{B}(X) - \mathcal{V}(X)$, where:

$$\mathcal{B}(X) = \begin{bmatrix} \delta AI + \sigma FI + \beta SI \\ dP + \theta F \\ \eta P + \varphi A \\ \omega P + b \\ \alpha S \\ \varepsilon I \end{bmatrix}, \mathcal{V}(X) = \begin{bmatrix} m_5 I \\ \delta AI + m_3 A \\ \sigma FI + m_4 F \\ \beta SI + m_1 S \\ m_2 P \\ \mu R \end{bmatrix}. \tag{9}$$

Determining the Jacobian matrices of (9), there are:

$$J\big(\mathcal{B}(X)\big) = \begin{bmatrix} \delta A + \sigma F + \beta S & \delta I & \sigma I & \beta I & 0 & 0 \\ 0 & 0 & \theta & 0 & d & 0 \\ 0 & \varphi & 0 & 0 & \eta & 0 \\ 0 & 0 & 0 & 0 & \omega & 0 \\ 0 & 0 & 0 & \alpha & 0 & 0 \\ \varepsilon & 0 & 0 & 0 & 0 & 0 \end{bmatrix}, \tag{10}$$

$$J\big(\mathcal{V}(X)\big) = \begin{bmatrix} m_5 & 0 & 0 & 0 & 0 & 0 \\ \delta A & \delta I + m_3 & 0 & 0 & 0 & 0 \\ \sigma F & 0 & \sigma I + m_4 & 0 & 0 & 0 \\ \beta S & 0 & 0 & \beta I + m_1 & 0 & 0 \\ 0 & 0 & 0 & 0 & m_2 & 0 \\ 0 & 0 & 0 & 0 & 0 & \mu \end{bmatrix}.$$

Selecting the submatrices related to the first four variables associated with infected individuals [38], the outcomes are indicated below:

$$B = \begin{bmatrix} f & 0 & 0 & 0 \\ 0 & 0 & \theta & 0 \\ 0 & \varphi & 0 & 0 \\ 0 & 0 & 0 & 0 \end{bmatrix}, V = \begin{bmatrix} m_5 & 0 & 0 & 0 \\ \frac{\alpha\delta b(dm_4+\theta\eta)}{(m_3m_4-\theta\varphi)(m_1m_2-\omega\alpha)} & m_3 & 0 & 0 \\ \frac{\alpha\sigma b(d\varphi+\eta m_3)}{(m_3m_4-\theta\varphi)(m_1m_2-\omega\alpha)} & 0 & m_4 & 0 \\ \frac{b\beta m_2}{m_1m_2-\omega\alpha} & 0 & 0 & m_1 \end{bmatrix}, \tag{11}$$

where $f = \frac{\delta\alpha b(dm_4+\theta\eta)+\sigma\alpha b(d\varphi+\eta m_3)+\beta b m_2(m_3m_4-\theta\varphi)}{(m_3m_4-\theta\varphi)(m_1m_2-\omega\alpha)}$.

By simple calculations, the next-generation matrix [39] is:

$$BV^{-1} = \begin{bmatrix} \frac{f}{m_5} & 0 & 0 & 0 \\ -\frac{\theta\alpha\sigma b(d\varphi+\eta m_3)}{m_4m_5(m_3m_4-\theta\varphi)(m_1m_2-\omega\alpha)} & 0 & \frac{\theta}{m_4} & 0 \\ -\frac{\alpha\varphi\delta b(dm_4+\theta\eta)}{m_3m_5(m_3m_4-\theta\varphi)(m_1m_2-\omega\alpha)} & \frac{\varphi}{m_3} & 0 & 0 \\ 0 & 0 & 0 & 0 \end{bmatrix}. \tag{12}$$

R_0 of the system (2) is the spectral radius of BV^{-1}, which is the characteristic root maximum of BV^{-1}. Clearly, R_0 is capable of being presented as:

$$R_0 = max\big\{\rho\big(BV^{-1}\big)\big\} = max\{R_{01}, R_{02}\}, \tag{13}$$

where $R_{01} = \frac{\delta\alpha b(dm_4+\theta\eta)+\sigma\alpha b(d\varphi+\eta m_3)+\beta b m_2(m_3m_4-\theta\varphi)}{m_5(m_3m_4-\theta\varphi)(m_1m_2-\omega\alpha)}$, $R_{02} = \sqrt{\frac{\varphi\theta}{m_3m_4}}$, and it is obvious that $R_{02} < 1$.

3.2 Stability of equilibrium points

Theorem 1 *If $R_{01} < 1$, the disease-free equilibrium point $E_0 = (S_1, P_1, A_1, F_1, I_1, R_1)$ is locally asymptotically stable.*

Proof For system (2), the Jacobian matrix at $E_0 = (S_1, P_1, A_1, F_1, I_1, R_1)$ can be written as:

$$J(E_0) = \begin{bmatrix} -m_1 & \omega & 0 & 0 & \frac{-b\beta m_2}{m_1m_2-\omega\alpha} & 0 \\ \alpha & -m_2 & 0 & 0 & 0 & 0 \\ 0 & d & -m_3 & \theta & \frac{-\delta\alpha b(dm_4+\theta\eta)}{(m_3m_4-\theta\varphi)(m_1m_2-\omega\alpha)} & 0 \\ 0 & \eta & \varphi & -m_4 & \frac{-\sigma\alpha b(t\eta m_3+d\varphi)}{(m_3m_4-\theta\varphi)(m_1m_2-\omega\alpha)} & 0 \\ 0 & 0 & 0 & 0 & m_5(R_{01}-1) & 0 \\ 0 & 0 & 0 & 0 & \varepsilon & -\mu \end{bmatrix}. \tag{14}$$

The characteristic equation for $J(E_0)$ is:

$$\begin{aligned}
&\left|\lambda E - J(E_0)\right| \\
&= (\lambda+\mu)\big(\lambda - m_5(R_{01}-1)\big)\left(\lambda + \frac{m_3+m_4}{2} + \frac{\sqrt{(m_3-m_4)^2+4\theta\varphi}}{2}\right) \\
&\quad \left(\lambda + \frac{m_3+m_4}{2} - \frac{\sqrt{(m_3-m_4)^2+4\theta\varphi}}{2}\right)\left(\lambda + \frac{m_1+m_2}{2} + \frac{\sqrt{(m_1-m_2)^2+4\alpha\omega}}{2}\right) \\
&\quad \left(\lambda + \frac{m_1+m_2}{2} - \frac{\sqrt{(m_1-m_2)^2+4\alpha\omega}}{2}\right).
\end{aligned} \tag{15}$$

The eigenvalues corresponding to the characteristic equation of $J(E_0)$ can be obviously obtained as:

$$\begin{aligned}
&\lambda_1 = -\mu < 0, \quad \lambda_2 = m_5(R_{01}-1), \\
&\lambda_3 = \frac{-\sqrt{(m_1+m_2)^2 - 4(m_1m_2-\omega\alpha)} - (m_1+m_2)}{2} < 0, \\
&\lambda_4 = \frac{\sqrt{(m_1+m_2)^2 - 4(m_1m_2-\omega\alpha)} - (m_1+m_2)}{2} < 0, \\
&\lambda_5 = \frac{-\sqrt{(m_3+m_4)^2 - 4(m_3m_4-\theta\varphi)} - (m_3+m_4)}{2} < 0, \\
&\lambda_6 = \frac{\sqrt{(m_3+m_4)^2 - 4(m_3m_4-\theta\varphi)} - (m_3+m_4)}{2} < 0.
\end{aligned} \tag{16}$$

If $R_{01} < 1$, there exists $\lambda_2 < 0$. By the Routh–Hurwitz stability criterion, if $R_{01} < 1$, E_0 is locally asymptotically stable. □

Theorem 2 *If $R_{01} > 1$ and $\beta m_2 m_5(\sigma m_3 + \delta m_4) + \delta\sigma(m_5(m_1m_2 - \omega\alpha)) > \delta\sigma b\beta m_2$, the disease-free equilibrium point $E_0 = (S_1, P_1, A_1, F_1, I_1, R_1)$ is locally asymptotically stable.*

Proof On the basis of equations (7), let $I \neq 0$, according to simple calculations, S^*, P^*, A^*, F^*, R^* can be, respectively, expressed by I^*, which is the nonnegative real root of the cubic equation $a_1I^3 + a_2I^2 + a_3I + a_4 = 0$, where:

$$\begin{aligned}
a_1 &= \delta\sigma\beta m_2 m_5, \\
a_2 &= \beta m_2 m_5(\sigma m_3 + \delta m_4) + \delta\sigma\big(m_5(m_1m_2 - \omega\alpha) - b\beta m_2\big), \\
a_3 &= (\delta m_4 + \sigma m_3)\big(m_5(m_1m_2 - \omega\alpha) - b\beta m_2\big) \\
&\quad + \beta m_2 m_5(m_3m_4 - \theta\varphi) - \alpha b\delta\sigma(d+\eta), \\
a_4 &= m_5(m_3m_4 - \theta\varphi)(m_1m_2 - \alpha\omega)(1 - R_{01}).
\end{aligned} \tag{17}$$

According to Cardan's formula and calculations, when $R_{01} > 1$ and $\beta m_2 m_5(\sigma m_3 + \delta m_4) + \delta\sigma(m_5(m_1m_2 - \omega\alpha)) > \delta\sigma b\beta m_2$, the cubic equation $a_1I^3 + a_2I^2 + a_3I + a_4 = 0$ has a non-

negative real root I^*, so E^* exists, the results are as follows:

$$\begin{aligned}
S^* &= \frac{bm_2}{(\beta I^* + m_1)m_2 - \alpha\omega}, P^* = \frac{\alpha b}{(\beta I^* + m_1)m_2 - \alpha\omega},\\
A^* &= \frac{\alpha b(d(\sigma I^* + m_4) + \theta\eta)}{((\beta I^* + m_1)m_2 - \alpha\omega)((\delta I^* + m_3)(\sigma I^* + m_4) - \varphi\theta)},\\
F^* &= \frac{\alpha b(\eta(\delta I^* + m_3) + \varphi d)}{((\beta I^* + m_1)m_2 - \alpha\omega)((\delta I^* + m_3)(\sigma I^* + m_4) - \varphi\theta)}, R^* = \frac{\varepsilon I^*}{\mu},\\
I^* &= \sqrt[3]{-\frac{27a_1^2a_4 - 9a_1a_2a_3 + 2a_2^3}{54a_1^3} + \sqrt{\frac{\frac{27}{4}a_1^2a_4^2 - \frac{9}{2}a_1a_2a_3a_4 - \frac{1}{4}a_2^2a_3^2 + a_2^3a_4 + a_1a_3^3}{27a_1^4}}}\\
&\quad + \sqrt[3]{-\frac{27a_1^2a_4 - 9a_1a_2a_3 + 2a_2^3}{54a_1^3} - \sqrt{\frac{\frac{27}{4}a_1^2a_4^2 - \frac{9}{2}a_1a_2a_3a_4 - \frac{1}{4}a_2^2a_3^2 + a_2^3a_4 + a_1a_3^3}{27a_1^4}}}.
\end{aligned} \tag{18}$$

Due to the complexity of the parameters in model (2), it is highly challenging to rigorously prove its local asymptotic stability at E^* theoretically. Therefore, this paper employs numerical solutions to explore the local asymptotic stability of the model. By substituting specific parameters into the model, a set of numerical solutions was successfully obtained, which satisfy the fundamental assumptions of the model, the results are as follows:

$$\begin{aligned}
&b = 0.00752, \alpha = 0.3, \omega = 0.3, \varphi = 0.2, \theta = 0.2, d = 0.3, \eta = 0.3,\\
&\beta = 0.4, \delta = 0.3, \sigma = 0.5, \varepsilon = 0.1270, \phi = 0.0001, \mu = 0.0074
\end{aligned} \tag{19}$$

and

$$\begin{aligned}
&S^* = 0.0303, P^* = 0.0113, A^* = 0.1546,\\
&F^* = 0.1519, I^* = 0.0368, R^* = 0.6308.
\end{aligned} \tag{20}$$

By calculating, all parameters that satisfy $R_{01} = 2.9866 > 1$ and $\beta m_2 m_5(\sigma m_3 + \delta m_4) + \delta\sigma(m_5(m_1m_2 - \omega\alpha)) - \delta\sigma b\beta m_2 > 0$. Also, through Fig. 3, at the positive equilibrium point E^*, model (2) is locally asymptotically stable. Apart from the set of parameters in this paper, there may exist other numerical solutions. This paper only discusses the sufficient condition for the model to satisfy local asymptotic stability. □

Theorem 3 *If $b(\delta + \sigma + \beta) < \phi\mu$, the disease-free equilibrium point $E_0 = (S_1, P_1, A_1, F_1, I_1, R_1)$ is globally asymptotically stable.*

Proof Constructing a Lyapunov function $K(t) = I(t) + R(t)$, and

$$\begin{aligned}
K'(t) =& I'(t) + R'(t)\\
=& \delta AI + \sigma FI + \beta SI - (\mu + \phi)I - \mu R\\
=& (\delta A + \sigma F + \beta S - \phi)I - \mu(I + R).
\end{aligned} \tag{21}$$

According to the positive invariant set (6), there exists $K'(t) \le (\frac{(\delta+\sigma+\beta)b}{\mu} - \phi)I - \mu(I + R)$. It can be seen that $K'(t) \le 0$ if and only if $b(\delta + \sigma + \beta) \le \mu\phi$, meanwhile, $K'(t) = 0$ if and only

if $S(t) = S_1$, $P(t) = P_1$, $A(t) = A_1$, $F(t) = F_1$, $I(t) = R(t) = 0$. That is, E_0 is the unique solution in the invariant set (6). Based on the Lyapunov–LaSalle Invariance Principle [40], it can be shown that the disease-free equilibrium point E_0 of system (2) is globally asymptotically stable if $b(\delta + \sigma + \beta) < \phi\mu$. □

Theorem 4 *If* $R_{01} > 1$ *and* $\beta m_2 m_5(\sigma m_3 + \delta m_4) + \delta\sigma(m_5(m_1 m_2 - \omega\alpha)) > \delta\sigma b\beta m_2$, *the positive equilibrium point* $E^* = (S^*, P^*, A^*, F^*, I^*, R^*)$ *is globally asymptotically stable*.

Proof Formulating a Lyapunov function:

$$\begin{aligned} C(t) = \big[&\big(S(t) - S^*\big) + \big(P(t) - P^*\big) + \big(A(t) - A^*\big) + \big(F(t) - F^*\big) + \big(I(t) - I^*\big) \\ &+ \big(R(t) - R^*\big)\big]^2 \end{aligned} \tag{22}$$

and

$$\begin{aligned} C'(t) =& 2\big[\big(S(t) - S^*\big) + \big(P(t) - P^*\big) + \big(A(t) - A^*\big) + \big(F(t) - F^*\big) + \big(I(t) - I^*\big) \\ &+ \big(R(t) - R^*\big)\big]\big[S'(t) + P'(t) + A'(t) + F'(t) + I'(t) + R'(t)\big]. \end{aligned} \tag{23}$$

Since E^* obeys equation (7), there is $b - \mu S^* - \mu P^* - \mu A^* - \mu F^* - \mu I^* - \mu R^* = 0$, that is $b = \mu S^* + \mu P^* + \mu A^* + \mu F^* + \mu I^* + \mu R^*$. Equation (23) can be evaluated as:

$$\begin{aligned} C'(t) =& 2\big[\big(S(t) - S^*\big) + \big(P(t) - P^*\big) + \big(A(t) - A^*\big) + \big(F(t) - F^*\big) + \big(I(t) - I^*\big) \\ &+ \big(R(t) - R^*\big)\big]\big[\mu\big(S^* - S(t)\big) + \mu\big(P^* - P(t)\big) + \mu\big(A^* - A(t)\big) \\ &+ \mu\big(F^* - F(t)\big) + \mu\big(I^* - I(t)\big) + \mu\big(R^* - R(t)\big)\big] \\ =& -2\mu\big[\big(S(t) - S^*\big) + \big(P(t) - P^*\big) + \big(A(t) - A^*\big) + \big(F(t) - F^*\big) \\ &+ \big(I(t) - I^*\big) + \big(R(t) - R^*\big)\big]^2 \\ \le& 0, \end{aligned} \tag{24}$$

where $C'(t) = 0$ if and only if $S = S^*$, $P = P^*$, $A = A^*$, $F = F^*$, $I = I^*$, $R = R^*$. In accordance with the Lyapunov–LaSalle Invariance Principle [40], system (2) is globally asymptotically stable at $E^* = (S^*, P^*, A^*, F^*, I^*, R^*)$. □

Moreover, the stability analysis of equilibrium points indicates that, in the biological system, even under complex behavioral responses and pseudoinfection phenomena, appropriate control measures can effectively maintain the dominance of the healthy population. This provides a theoretical foundation for optimizing control strategy.

4 The optimal control model

This paper considers applying the model to a closed environment, such as a school campus, and proposes four control objectives over a certain control time interval. On the one hand, the aim is to increase the alert population while reducing the number of fragile individuals following pseudoinfection. On the other hand, this paper aims to reduce the scale of the transition to the infectious state. This paper introduces time-dependent control variables $\chi_1(t)$ and $\chi_2(t)$, which represent the effects of positive prevention education and community encouragement guidance. The control measures will be ineffective if

$\chi_1(t) = \chi_2(t) = 0$, and fully effective if $\chi_1(t) = \chi_2(t) = 1$, where $1 - \chi_1(t)$ represents the effect of suppressing the transition of alert individuals to the fragile state, and $1 - \chi_2(t)$ represents the effect of suppressing the transition of alert individuals to the infectious state. We further change the proportion constants d, θ in the model (2) to be control variables $d(t)$ and $\theta(t)$, which are used to control the proportion of alert individuals with pseudoinfection and fragile individuals, respectively. The proportion of alert individuals with pseudoinfected symptoms in a closed environment can be increased by actively promoting prevention education and encouraging guidance in the community. The system augmented with control is given by:

$$\begin{cases} \frac{dS}{dt} = b - m_1 S - \beta SI + \omega P, \\ \frac{dP}{dt} = \alpha S - m_2 P, \\ \frac{dA}{dt} = d(t)P - (1 - \chi_2(t))\delta AI + \theta(t)F - (1 - \chi_1(t))\varphi A - \mu A, \\ \frac{dF}{dt} = \eta P - \sigma FI + (1 - \chi_1(t))\varphi A - \theta(t)F - \mu F, \\ \frac{dI}{dt} = (1 - \chi_2(t))\delta AI + \sigma FI + \beta SI - m_5 I, \\ \frac{dR}{dt} = \varepsilon I - \mu R. \end{cases} \tag{25}$$

The objective is to maximize the proportion of alert individuals with pseudoinfected symptoms within a limited time frame, while minimizing the proportion of fragile individuals, reducing the scale of transition to the infectious state, and ultimately containing the spread of the virus. The objective function has the form:

$$J(\chi_1, \chi_2, d, \theta) = \int_{t_0}^{T} \left[DA(t) - \frac{c_1}{2}\chi_1^2(t) - \frac{c_2}{2}\chi_2^2(t) - \frac{c_3}{2}d^2(t) - \frac{c_4}{2}\theta^2(t) \right] dt, \tag{26}$$

where

$$\begin{aligned} &\chi_1(t), \chi_2(t), d(t), \theta(t) \in U \triangleq \{(\chi_1, \chi_2, d, \theta) | \chi_1(t), \chi_2(t), d(t), \theta(t) \textit{are} \\ &\quad \textit{measurable, and } 0 \le \chi_1(t), \chi_2(t), d(t), \theta(t) \le 1, \forall t \in [t_0, T]\} \end{aligned} \tag{27}$$

and t_0 is the initial control time, U is the allowable control set, T is the end control time, c_i $(i = 1, 2, 3, 4)$ is the weighting coefficient of the control variable, and D is the weighting coefficient of the alert individuals, the square of the controlling variables reflects the effects of proactive preventive education and community encouragement and guidance. System (25) satisfies the initial condition (4).

Theorem 5 *There exists an optimal four-dimensional control pair* $(\chi_1^*(t), \chi_2^*(t), d^*(t), \theta^*(t)) \in U$, *thus creating the following function*:

$$J\left(\chi_1^*, \chi_2^*, d^*, \theta^*\right) = \max J(\chi_1, \chi_2, d, \theta), \chi_1(t), \chi_2(t), d(t), \theta(t) \in U. \tag{28}$$

Proof Proving that optimal control exists requires only five conditions:

- The state variables and control variables are both nonnegative.
- The admissible control set U is both closed and convex.
- The convex integral function is defined within the allowed set U.

- In the system (25), the expressions on the right-hand side are functions that are related to control and state variables, and are linear and bounded.
- There exist positive numbers $a_1, a_2 > 0$, and $a_3 > 0$ such that the integrand expression $L(t, A(t), \chi_1, \chi_2, d, \theta) = DA(t) - \frac{c_1}{2}\chi_1^2(t) - \frac{c_2}{2}\chi_2^2(t) - \frac{c_3}{2}d^2(t) - \frac{c_4}{2}\theta^2(t)$ in the target functional satisfies $-L(t, A(t), \chi_1, \chi_2, d, \theta) \geq a_1(|\chi_1|^2 + |\chi_2|^2 + |d|^2 + |\theta|^2)^{a_2/2} - a_3$.

The first three conditions are evidently satisfied, and it suffices to verify the last two. According to the positive invariant set (6), it follows that:

$$\frac{b}{\mu} \geq \max\{S(t), P(t), A(t), F(t), I(t), R(t)\} \tag{29}$$

and the right end of system (25) satisfies the following inequalities:

$$\begin{aligned} &\frac{dS}{dt} \leq b, \frac{dP}{dt} \leq \frac{\alpha b}{\mu}, \frac{dA}{dt} \leq d(t)P + \theta(t)F, \frac{dF}{dt} \leq \frac{b\eta}{\mu} + \big(1 - \chi_1(t)\big)\varphi A, \\ &\frac{dI}{dt} \leq (\sigma + \beta)\frac{b^2}{\mu^2} + \big(1 - \chi_2(t)\big)\delta AI, \frac{dR}{dt} \leq \frac{\varepsilon b}{\mu}. \end{aligned} \tag{30}$$

Therefore, the fourth condition holds. Furthermore, by the positive invariant set (6), there is:

$$\begin{aligned} -L\big(t, A(t), \chi_1, \chi_2, d, \theta\big) =& \frac{c_1}{2}\chi_1^2(t) + \frac{c_2}{2}\chi_2^2(t) + \frac{c_3}{2}d^2(t) + \frac{c_4}{2}\theta^2(t) - DA(t) \\ \geq& \frac{c_1}{2}\chi_1^2(t) + \frac{c_2}{2}\chi_2^2(t) + \frac{c_3}{2}d^2(t) + \frac{c_4}{2}\theta^2(t) - \frac{Db}{\mu}. \end{aligned} \tag{31}$$

Let $a_1 = \min\{\frac{c_1}{2}, \frac{c_2}{2}, \frac{c_3}{2}, \frac{c_4}{2}\}$, $a_2 = 2$, and $a_3 = \frac{Db}{\mu}$, so that the inequality is established below:

$$-L\big(t, A(t), \chi_1, \chi_2, d, \theta\big) \geq a_1\big(|\chi_1|^2 + |\chi_2|^2 + |d|^2 + |\theta|^2\big)^{a_2/2} - a_3. \tag{32}$$

The last condition holds, and therefore, optimal control can be achieved.

To address the multiple complex constraints in the model (25), such as the nonnegativity and range limitations of control and state variables, and to achieve effective tradeoffs in multiobjective optimization, the augmented Hamiltonian is introduced. Compared to the standard Hamiltonian, the augmented Hamiltonian incorporates penalty terms, enabling a more systematic integration of constraints and objectives while satisfying the Pontryagin maximum principle under more general conditions. Based on the Pontryagin maximum principle, this paper defines a Hamiltonian function with penalty terms, which leads to an expression for the optimal control system. The augmented Hamiltonian can be represented as:

$$\begin{aligned} H =& -DA(t) + \frac{c_1}{2}\chi_1^2(t) + \frac{c_2}{2}\chi_2^2(t) + \frac{c_3}{2}d^2(t) + \frac{c_4}{2}\theta^2(t) \\ &+ \varkappa_1(t)[b - m_1 S - \beta SI + \omega P] + \varkappa_2(t)[\alpha S - m_2 P] \\ &+ \varkappa_3(t)\big[d(t)P + \theta(t)F - \mu A - \big(1 - \chi_2(t)\big)\delta AI - \big(1 - \chi_1(t)\big)\varphi A\big] \\ &+ \varkappa_4(t)\big[\eta P - \sigma FI + \big(1 - \chi_1(t)\big)\varphi A - \theta(t)F - \mu F\big] \\ &+ \varkappa_5(t)\big[\big(1 - \chi_2(t)\big)\delta AI + \sigma FI + \beta SI - m_5 I\big] + \varkappa_6(t)[\varepsilon I - \mu R] \end{aligned} \tag{33}$$

$$
\begin{aligned}
&- \varrho_{11}(t)\chi_1(t) - \varrho_{12}(t)\big(1-\chi_1(t)\big) - \varrho_{21}(t)\chi_2(t)\\
&- \varrho_{22}(t)\big(1-\chi_2(t)\big) - \varrho_{31}(t)d(t) - \varrho_{32}(t)\big(1-d(t)\big)\\
&- \varrho_{41}(t)\theta(t) - \varrho_{42}(t)\big(1-\theta(t)\big),
\end{aligned}
$$

where $\varkappa_i(t)$ $(i = 1,2,3,4,5,6)$ is an adjoint variable and $\varrho_{ij}(t) \geq 0$ $(i = 1,2,3,4,\ j = 1,2)$ denotes the penalty operator, which satisfies that $\varrho_{11}(t)\chi_1(t) = \varrho_{12}(t)(1-\chi_1(t)) = 0$ at optimal control χ_1^*, $\varrho_{21}(t)\chi_2(t) = \varrho_{22}(t)(1-\chi_2(t)) = 0$ at optimal control χ_2^*, $\varrho_{31}(t)d(t) = \varrho_{32}(t)(1-d(t)) = 0$ at optimal control d^*, and $\varrho_{41}(t)\theta(t) = \varrho_{42}(t)(1-\theta(t)) = 0$ at optimal control θ^*. □

Theorem 6 *For the optimal control pair* $(\chi_1^*(t), \chi_2^*(t), d^*(t), \theta^*(t)) \in U$ *and the solution* $(S(t), P(t), A(t), F(t), I(t), R(t)) \in \mathbb{R}_+^6$ *for state system* (25)*, adjoint variables* $\varkappa_1(t)$*,* $\varkappa_2(t)$*,* $\varkappa_3(t)$*,* $\varkappa_4(t)$*,* $\varkappa_5(t)$*, and* $\varkappa_6(t)$ *satisfy the given conditions*:

$$
\begin{cases}
\dfrac{d\varkappa_1}{dt} = (m_1 + \beta I)\varkappa_1(t) - \alpha\varkappa_2(t) - \beta I\varkappa_5(t),\\
\dfrac{d\varkappa_2}{dt} = m_2\varkappa_2(t) - \omega\varkappa_1(t) - d(t)\varkappa_3(t) - \eta\varkappa_4(t),\\
\dfrac{d\varkappa_3}{dt} = \big(\varkappa_3(t) - \varkappa_4(t)\big)\big(1-\chi_1(t)\big)\varphi + \big(\varkappa_3(t) - \varkappa_5(t)\big)\big(1-\chi_2(t)\big)\delta I\\
\qquad\qquad + \varkappa_3(t)\mu + D,\\
\dfrac{d\varkappa_4}{dt} = \big(\varkappa_4(t) - \varkappa_3(t)\big)\theta(t) + \varkappa_4(t)\mu - \varkappa_5(t)\sigma I,\\
\dfrac{d\varkappa_5}{dt} = \big(\varkappa_1(t) - \varkappa_5(t)\big)\beta S + \big(\varkappa_3(t) - \varkappa_5(t)\big)\big(1-\chi_2(t)\big)\delta A\\
\qquad\qquad + \big(\varkappa_4(t) - \varkappa_5(t)\big)\sigma F + \varkappa_5(t)m_5 - \varkappa_6(t)\varepsilon,\\
\dfrac{d\varkappa_6}{dt} = \varkappa_6(t)\mu.
\end{cases}
\tag{34}
$$

The boundary conditions are:

$$
\varkappa_1(T) = \varkappa_2(T) = \varkappa_3(T) = \varkappa_4(T) = \varkappa_5(T) = \varkappa_6(T) = 0. \tag{35}
$$

The expressions for optimal control variables of the state system (25) *can be given by the following formulas*:

$$
\begin{aligned}
\chi_1^*(t) &= \min\left\{1, \max\left\{0, \frac{(\varkappa_4(t) - \varkappa_3(t))\varphi A}{c_1}\right\}\right\},\\
\chi_2^*(t) &= \min\left\{1, \max\left\{0, \frac{(\varkappa_5(t) - \varkappa_3(t))\delta AI}{c_2}\right\}\right\},\\
d^*(t) &= \min\left\{1, \max\left\{0, \frac{-\varkappa_3(t)P}{c_3}\right\}\right\},\\
\theta^*(t) &= \min\left\{1, \max\left\{0, \frac{(\varkappa_4(t) - \varkappa_3(t))F}{c_4}\right\}\right\}.
\end{aligned}
\tag{36}
$$

Proof The adjoint system can be expressed on the basis of the Pontryagin maximum principle as follows:

$$\begin{aligned} &\frac{d\varkappa_1}{dt} = -\frac{\partial H}{\partial S}, \frac{d\varkappa_2}{dt} = -\frac{\partial H}{\partial P}, \frac{d\varkappa_3}{dt} = -\frac{\partial H}{\partial A}, \\ &\frac{d\varkappa_4}{dt} = -\frac{\partial H}{\partial F}, \frac{d\varkappa_5}{dt} = -\frac{\partial H}{\partial I}, \frac{d\varkappa_6}{dt} = -\frac{\partial H}{\partial R} \end{aligned} \tag{37}$$

and the boundary condition for the adjoint system is (35).

To obtain the optimality condition, the Hamiltonian function takes the derivative of the control variables $\chi_1(t)$, $\chi_2(t)$, $d(t)$, and $\theta(t)$, respectively, to obtain:

$$\begin{aligned} \frac{\partial H}{\partial \chi_1} =& c_1\chi_1(t) + \big(\varkappa_3(t) - \varkappa_4(t)\big)\varphi A - \varrho_{11} + \varrho_{12}, \\ \frac{\partial H}{\partial \chi_2} =& c_2\chi_2(t) + \big(\varkappa_3(t) - \varkappa_5(t)\big)\delta AI - \varrho_{21} + \varrho_{22}, \\ \frac{\partial H}{\partial d} =& c_3 d(t) + \varkappa_3(t)P - \varrho_{31} + \varrho_{32}, \\ \frac{\partial H}{\partial \theta} =& c_4\theta(t) + \big(\varkappa_3(t) - \varkappa_4(t)\big)F - \varrho_{41} + \varrho_{42} \end{aligned} \tag{38}$$

and set them equal to 0; the optimal control formulas are as follows:

$$\begin{aligned} \chi_1^*(t) =& \frac{(\varkappa_4(t) - \varkappa_3(t))\varphi A + \varrho_{11} - \varrho_{12}}{c_1}, \\ \chi_2^*(t) =& \frac{(\varkappa_5(t) - \varkappa_3(t))\delta AI + \varrho_{21} - \varrho_{22}}{c_2}, \\ d^*(t) =& \frac{-\varkappa_3(t)P + \varrho_{31} - \varrho_{32}}{c_3}, \\ \theta^*(t) =& \frac{(\varkappa_4(t) - \varkappa_3(t))F + \varrho_{41} - \varrho_{42}}{c_4}. \end{aligned} \tag{39}$$

To derive the ultimate optimal control equations without punitive conditions, this paper examines the subsequent three scenarios taking $\chi_1^*(t)$ as an illustrative example:

- In the set $\{t|0 < \chi_1^*(t) < 1\}$, the first scenario occurs when $\varrho_{11}(t) = \varrho_{12}(t) = 0$. Subsequently, the optimal control formula is:

$$\chi_1^*(t) = \frac{(\varkappa_4(t) - \varkappa_3(t))\varphi A}{c_1}. \tag{40}$$

- If $\varrho_{11}(t) = 0$ in $\{t|\chi_1^*(t) = 1\}$, then the optimum control formula can be expressed as:

$$1 = \chi_1^*(t) = \frac{(\varkappa_4(t) - \varkappa_3(t))\varphi A - \varrho_{12}}{c_1}, \tag{41}$$

due to $\varrho_{12}(t) \geq 0$, which means that $\frac{(\varkappa_4(t)-\varkappa_3(t))\varphi A}{c_1} \geq 1$.

- If $\varrho_{12}(t) = 0$ in the set $\{t \mid \chi_1^*(t) = 0\}$, the formula for the optimal control is given by:

$$0 = \chi_1^*(t) = \frac{(\varkappa_4(t) - \varkappa_3(t))\varphi A + \varrho_{11}}{c_1}, \tag{42}$$

due to $\varrho_{11}(t) \geq 0$, which means that $\frac{(\varkappa_4(t)-\varkappa_3(t))\varphi A}{c_1} \leq 0$.

On the basis of the given situation, the ultimate formula for optimal control of $\chi_1^*(t)$ is:

$$\chi_1^*(t) = \min\left\{1, \max\left\{0, \frac{(\varkappa_4(t) - \varkappa_3(t))\varphi A}{c_1}\right\}\right\}. \tag{43}$$

Similarly, the ultimate control formulas for $\chi_2^*(t)$, $d^*(t)$, and $\theta^*(t)$ are given by:

$$\begin{aligned}
\chi_2^*(t) &= \min\left\{1, \max\left\{0, \frac{(\varkappa_5(t) - \varkappa_3(t))\delta AI}{c_2}\right\}\right\},\\
d^*(t) &= \min\left\{1, \max\left\{0, \frac{-\varkappa_3(t)P}{c_3}\right\}\right\},\\
\theta^*(t) &= \min\left\{1, \max\left\{0, \frac{(\varkappa_4(t) - \varkappa_3(t))F}{c_4}\right\}\right\}.
\end{aligned} \tag{44}$$

In this optimal control system, the state system (25) and adjoint system (34) work together, satisfying initial, boundary, and optimal conditions to achieve the best control. The optimal control system is represented by:

$$\begin{cases}
\frac{dS}{dt} = b - m_1 S - \beta SI + \omega P,\\
\frac{dP}{dt} = \alpha S - m_2 P,\\
\frac{dA}{dt} = d^*(t)P - \big(1 - \chi_2^*(t)\big)\delta AI + \theta^*(t)F - \big(1 - \chi_1^*(t)\big)\varphi A - \mu A,\\
\frac{dF}{dt} = \eta P - \sigma FI + \big(1 - \chi_1^*(t)\big)\varphi A - \theta^*(t)F - \mu F,\\
\frac{dI}{dt} = \big(1 - \chi_2^*(t)\big)\delta AI + \sigma FI + \beta SI - m_5 I,\\
\frac{dR}{dt} = \varepsilon I - \mu R,\\
\frac{d\varkappa_1}{dt} = (m_1 + \beta I)\varkappa_1(t) - \alpha\varkappa_2(t) - \beta I\varkappa_5(t),\\
\frac{d\varkappa_2}{dt} = m_2\varkappa_2(t) - \omega\varkappa_1(t) - d(t)\varkappa_3(t) - \eta\varkappa_4(t),\\
\frac{d\varkappa_3}{dt} = \big(\varkappa_3(t) - \varkappa_4(t)\big)\big(1 - \chi_1(t)\big)\varphi + \big(\varkappa_3(t) - \varkappa_5(t)\big)\big(1 - \chi_2(t)\big)\delta I + \varkappa_3(t)\mu + D,\\
\frac{d\varkappa_4}{dt} = \big(\varkappa_4(t) - \varkappa_3(t)\big)\theta(t) + \varkappa_4(t)\mu - \varkappa_5(t)\sigma I,\\
\frac{d\varkappa_5}{dt} = \big(\varkappa_1(t) - \varkappa_5(t)\big)\beta S + \big(\varkappa_3(t) - \varkappa_5(t)\big)\big(1 - \chi_2(t)\big)\delta A + \big(\varkappa_4(t) - \varkappa_5(t)\big)\sigma F\\
\qquad + \varkappa_5(t)m_5 - \varkappa_6(t)\varepsilon,\\
\frac{d\varkappa_6}{dt} = \varkappa_6(t)\mu,\\
S(t_0) = S^0, P(t_0) = P^0, A(t_0) = A^0, F(t_0) = F^0, I(t_0) = I^0, R(t_0) = R^0,\\
\varkappa_1(T) = \varkappa_2(T) = \varkappa_3(T) = \varkappa_4(T) = \varkappa_5(T) = \varkappa_6(T) = 0.
\end{cases} \tag{45}$$

□

The analysis of the optimal control system highlights the critical role of proactive prevention education and community interventions in reducing the vulnerable population and controlling the scale of infection. By introducing a Hamiltonian function with penalty terms, we optimized the dynamic adjustment strategy for control variables. Biologically, this indicates that rational allocation of resources to maximize the proportion of alert individuals while minimizing the transition rate to the infected population can significantly enhance the efficiency of disease control.

5 The stochastic model

On the basis of the deterministic SPAFIR model, further consideration has been given to the impact of stochastic factors on the infectious disease. The effective contact rates δ and σ directly influence the speed and scale of disease transmission, making them critical parameters in describing the dynamics of infectious disease spread. Variations in δ and σ significantly affect the system's dynamic characteristics, such as the peak number of infections, transmission rate, and overall outbreak size. Therefore, this paper assumes that the effective contact rates δ and σ are subject to stochastic perturbations; let $\delta + \rho_1 \dot{W}_1(t)$ and $\sigma + \rho_2 \dot{W}_2(t)$, respectively, represent the random disturbances of the effective contact rates, they are incorporated into the model (2) to obtain the corresponding disturbed system:

$$\begin{cases} dS(t) = \big(b - m_1 S(t) - \beta S(t) I(t) + \omega P(t)\big)dt, \\ dP(t) = \big(\alpha S(t) - m_2 P(t)\big)dt, \\ dA(t) = \big(dP(t) - \delta A(t) I(t) + \theta F(t) - m_3 A(t)\big)dt - \rho_1 A(t) I(t) dW_1(t), \\ dF(t) = \big(\eta P(t) - \sigma F(t) I(t) + \varphi A(t) - m_4 F(t)\big)dt - \rho_2 F(t) I(t) dW_2(t), \\ dI(t) = \big(\delta A(t) I(t) + \sigma F(t) I(t) + \beta S(t) I(t) - m_5 I(t)\big)dt + \rho_1 A(t) I(t) dW_1(t) \\ \qquad + \rho_2 F(t) I(t) dW_2(t), \\ dR(t) = \big(\varepsilon I(t) - \mu R(t)\big)dt, \end{cases} \tag{46}$$

where $W_1(t)$ and $W_2(t)$ are independently standard Brownian motions, the instant at which the initial value is zero, namely $W_1(0) = W_2(0) = 0$. ρ_i^2 represents the corresponding disturbance intensity, and $\dot{W}_i(t)$ denotes white noise, where $i = 1, 2$.

6 Stochastic model analysis

Theorem 7 *For any given initial value* $(S^0, P^0, A^0, F^0, I^0, R^0) \in \mathbb{R}_+^6$ *and* $t \geq 0$, *system* (46) *exists a unique positive solution, which exists in* $\mathbb{R}_+^6$ *with probability* 1, *a.s.*

Proof Assuming that there is $I = e^{v(t)}$, then $v(t) = \ln I$, and utilizing *Itô's* formula, there is $dv(t) = \frac{1}{I} dI - \frac{1}{2I^2}(dI)^2$, model (47) can be obtained as:

$$\begin{cases} dS(t) = \big(b - m_1 S(t) - \beta S(t) e^{v(t)} + \omega P(t)\big)dt, \\ dP(t) = \big(\alpha S(t) - m_2 P(t)\big)dt, \\ dA(t) = \big(dP(t) - \delta A(t) e^{v(t)} + \theta F(t) - m_3 A(t)\big)dt - \rho_1 A(t) e^{v(t)} dW_1(t), \\ dF(t) = \big(\eta P(t) - \sigma F(t) e^{v(t)} + \varphi A(t) - m_4 F(t)\big)dt - \rho_2 F(t) e^{v(t)} dW_2(t), \\ dv(t) = \left(\delta A(t) + \sigma F(t) + \beta S(t) - m_5 - \dfrac{\rho_1^2 A^2 + \rho_2^2 F^2}{2}\right)dt \\ \qquad + \rho_1 A(t) dW_1(t) + \rho_2 F(t) dW_2(t), \\ dR(t) = \big(\varepsilon e^{v(t)} - \mu R(t)\big)dt. \end{cases} \tag{47}$$

The models (47) and (46) are equivalent, and the coefficients in model (47) are locally *Lipschitz* continuous. Therefore, in the time interval $[0, \tau_b)$, there exists a unique local solution $(S(t), P(t), A(t), F(t), I(t), R(t))$ for any initial condition $(S^0, P^0, A^0, F^0, I^0, R^0)$, where τ_b is the blasting time. For the proof that this solution is global, it is sufficient to show that $\tau_b = +\infty$. Assuming that there exists $m \geq g_0 \geq 1$ such that the initial state stays within the interval $[\frac{1}{g}, g_0]$, the stopping time τ_g is defined as:

$$\begin{aligned}\tau_g = inf\Big\{ & t \in [0, \tau_b) : \min\big(S(t), P(t), A(t), F(t), I(t), R(t)\big) \leq \frac{1}{g} \ or \\ & \max\big(S(t), P(t), A(t), F(t), I(t), R(t)\big) \geq g\Big\}.\end{aligned} \tag{48}$$

We set $inf\,\Phi = +\infty$, where Φ is an empty set. In accordance with the stopping-time definition, it can be deduced that τ_g is a function that increases monotonically with g. Therefore, there exists $\lim_{g\to\infty} \tau_g = \tau_\infty$, and it is obvious that $\tau_\infty \leq \tau_b, a.s.$. For all $t \geq 0$, there exist $\tau_b = +\infty$ and $(S(t), P(t), A(t), F(t), I(t), R(t)) \in \mathbb{R}^6_+$ if it can be demonstrated that $\tau_\infty = +\infty$, a.s. The next task is to prove, through a contradiction, that $\tau_\infty = +\infty$. Assuming $\tau_\infty \neq +\infty$, $\Upsilon > 0$ and a very small value $\varsigma > 0$ such that $P(\tau_\infty < \Upsilon) > \varsigma$. Since the function τ_g increases monotonically, it is possible to derive $P(\tau_g < \Upsilon) > \varsigma$. Let $f(y) = y - 1 - \ln y$, define the function:

$$V(S, P, A, F, I, R) = f(S) + f(P) + f(A) + f(F) + f(I) + f(R). \tag{49}$$

For any $t \in [0, \tau_g)$, using *Itô's* formula, it can be obtained that:

$$\begin{aligned} dV(S,P,A,F,I,R) = & \left(1 - \frac{1}{S}\right)dS + \frac{1}{2S^2}(dS)^2 + \left(1 - \frac{1}{P}\right)dP + \frac{1}{2P^2}(dP)^2 \\ & + \left(1 - \frac{1}{A}\right)dA + \frac{1}{2A^2}(dA)^2 + \left(1 - \frac{1}{F}\right)dF + \frac{1}{2F^2}(dF)^2 \\ & \left(1 - \frac{1}{I}\right)dI + \frac{1}{2I^2}(dI)^2 + \left(1 - \frac{1}{R}\right)dR + \frac{1}{2R^2}(dR)^2 \\ = & \big(b - \phi I - \mu(S + P + A + F + I + R)\big)dt - \left(\frac{b}{S} - m_1\right. \\ & \left. - \beta I + \omega P\right)dt - \left(\frac{\alpha S}{P} - m_2\right)dt - \left(\frac{dP}{A} - \delta I + \frac{\theta F}{A} - m_3\right. \\ & \left. - \frac{\rho_1^2 I^2}{2}\right)dt + \rho_1 I dW_1 - \left(\frac{\eta P}{F} - \sigma I + \frac{\varphi A}{F} - m_4 - \frac{\rho_2^2 I^2}{2}\right)dt \\ & + \rho_2 I dW_2 - \left(\delta A + \sigma F + \beta S - m_5 - \frac{\rho_1^2 A^2 + \rho_2^2 F^2}{2}\right)dt \\ & - \rho_1 A dW_1 - \rho_2 F dW_2 - \left(\frac{\varepsilon I}{R} - \mu\right)dt \\ = & \left(b - \mu(S + P + A + F + I + R) - \phi I - \left(\frac{b}{S} + \frac{\eta P}{F} + \frac{dP}{A}\right.\right. \\ & \left.\left. + \frac{\eta S}{P} + \frac{\varepsilon I}{R} - \frac{\theta F}{A} - \frac{\varphi A}{F}\right) + \mu + m_1 + m_2 + m_3 + m_4 + m_5\right. \end{aligned} \tag{50}$$

$$+\beta I+\delta I+\sigma I-\delta A-\sigma F-\beta S-\omega P+\frac{\rho_1^2(A^2+I^2)}{2}$$
$$+\frac{\rho_2^2(F^2+I^2)}{2}\Big)dt+\rho_1(I-A)dW_1+\rho_2(I-F)dW_2.$$

Setting that:

$$\begin{aligned}P=&b-\mu(S+P+A+F+I+R)-\phi I-\Big(\frac{b}{S}+\frac{\eta S}{P}+\frac{dP}{A}+\frac{\eta P}{F}\\&+\frac{\varepsilon I}{R}-\frac{\theta F}{A}-\frac{\varphi A}{F}\Big)+m_1+m_2+m_3+m_4+m_5+\mu+\beta I\\&+\delta I+\sigma I-\delta A-\sigma F-\beta S-\omega P+\frac{\rho_1^2(A^2+I^2)}{2}+\frac{\rho_2^2(F^2+I^2)}{2}\end{aligned}\tag{51}$$

and then there is:

$$\begin{aligned}P\le&b+\frac{\theta F}{A}+\frac{\varphi A}{F}+m_1+m_2+m_3+m_4+m_5+\mu+\beta I+\delta I+\sigma I\\&+\frac{\rho_1^2(A^2+I^2)}{2}+\frac{\rho_2^2(F^2+I^2)}{2}:=K.\end{aligned}\tag{52}$$

Therefore, it can be obtained that:

$$dV(S,P,A,F,I,R)\le Kdt+\rho_1(I-A)dW_1+\rho_2(I-F)dW_2.\tag{53}$$

Integrate t from 0 to τ_g on both sides of the inequality (53), taking the expectations of both sides, this can be represented as:

$$\begin{aligned}EV\big(S(\tau_g),P(\tau_g),A(\tau_g),F(\tau_g),I(\tau_g),R(\tau_g)\big)\le&EV\big(S^0,P^0,A^0,F^0,I^0,R^0\big)+KE(\tau_g)\\=&V\big(S^0,P^0,A^0,F^0,I^0,R^0\big)+K\tau_g\\\le&V\big(S^0,P^0,A^0,F^0,I^0,R^0\big)+K\Upsilon.\end{aligned}\tag{54}$$

Since $P(\tau_g<\Upsilon)>\varsigma$, it follows that for each $t\in\{\tau_g\le\Upsilon\}$, at least one of the quantities in $S(\tau_g)$, $P(\tau_g)$, $A(\tau_g)$, $F(\tau_g)$, $I(\tau_g)$, and $R(\tau_g)$ is equal to $\frac{1}{m}$ or m, there always exists:

$$\begin{aligned}&V(S(\tau_g\wedge\Upsilon),P(\tau_g\wedge\Upsilon),A(\tau_g\wedge\Upsilon),F(\tau_g\wedge\Upsilon),I(\tau_g\wedge\Upsilon),R(\tau_g\wedge\Upsilon))\\&\qquad\ge(g-1-\ln g)\wedge(\tfrac{1}{g}-1-\ln\tfrac{1}{g}).\end{aligned}\tag{55}$$

Combining (54) and (55), it can be obtained that:

$$\begin{aligned}V\big(S^0,P^0,A^0,F^0,I^0,R^0\big)+K\Upsilon\ge&E\big(1_{\{\tau_g\le\Upsilon\}}V\big(S(\tau_g\wedge\Upsilon),P(\tau_g\wedge\Upsilon),A(\tau_g\wedge\Upsilon),\\&F(\tau_g\wedge\Upsilon),I(\tau_g\wedge\Upsilon),R(\tau_g\wedge\Upsilon)\big)\big)\\\ge&\varsigma\cdot inf\Big\{\frac{1}{g}-1-\ln g\ or\ g-1+\ln g\Big\},\end{aligned}\tag{56}$$

where $1_{\{\tau_g \leq \Upsilon\}}$ is the indicative function for the set $\{\tau_g \leq \Upsilon\}$. Letting $g \to \infty$, it can be obtained that:

$$V\left(S^0, P^0, A^0, F^0, I^0, R^0\right) + K\Upsilon \geq \infty. \tag{57}$$

Meanwhile, for any initial condition $(S^0, P^0, A^0, F^0, I^0, R^0) \in \mathbb{R}^6_+$, it is easy to know that $V(S^0, P^0, A^0, F^0, I^0, R^0)$ is a real number, it can be derived as:

$$V\left(S^0, P^0, A^0, F^0, I^0, R^0\right) + K\Upsilon < \infty. \tag{58}$$

Equations (57) and (58) contradict each other, so the assumption is not valid. Hence, it is proved that $\tau_b = +\infty$, and thus model (46) has a globally unique positive solution with probability 1, a.s. □

Theorem 8 *If $R_0 > 1$ and for any initial condition $(S^0, P^0, A^0, F^0, I^0) \in R^5_+$ of system (61), satisfying the following conditions*:

$$0 < M < \min\left\{\xi_1 S^2, \xi_2 P^2, \xi_3 A^2, \xi_4 F^2, \xi_5 I^2\right\}, \tag{59}$$

where

$$\begin{aligned}
M =& \frac{1}{2}\rho_1^2 A^*\left(I^*\right)^2 + \frac{1}{2}\rho_2^2 F^*\left(I^*\right)^2 + \frac{1}{2}\rho_1^2 I^*\left(A^*\right)^2 + \frac{1}{2}\rho_2^2 I^*\left(F^*\right)^2,\\
\xi_1 =& \mu,\\
\xi_2 =& \mu,\\
\xi_3 =& \mu - \frac{1}{2}\rho_1^2 I^*,\\
\xi_4 =& \mu - \frac{1}{2}\rho_2^2 I^*,\\
\xi_5 =& \mu + \varepsilon - \frac{1}{2}\rho_1^2 A^* - \frac{1}{2}\rho_2^2 F^*.
\end{aligned} \tag{60}$$

The stationary distribution π exists for the model presented in equations (61). Moreover, the solution to the model is ergodic.

Proof Consider the first four equations of the model (47), forming the following random system:

$$\begin{cases}
dS(t) = \left(b - \beta S(t)I(t) - m_1 S(t) + \omega P(t)\right)dt,\\
dP(t) = \left(\alpha S(t) - m_2 P(t)\right)dt,\\
dA(t) = \left(dP(t) - \delta A(t)I(t) + \theta F(t) - m_3 A(t)\right)dt - \rho_1 A(t)I(t)dW_1(t),\\
dF(t) = \left(\eta P(t) - \sigma F(t)I(t) + \varphi A(t) - m_4 F(t)\right)dt - \rho_2 F(t)I(t)dW_2(t),\\
dI(t) = \left(\delta A(t)I(t) + \sigma F(t)I(t) + \beta S(t)I(t) - m_5 I(t)\right)dt + \rho_1 A(t)I(t)dW_1(t)\\
\qquad + \rho_2 F(t)I(t)dW_2(t).
\end{cases} \tag{61}$$

Define a C^2 function:

$$\Theta(S,P,A,F,I,R) = \Theta_1 + \Theta_2 + \Theta_3 + \Theta_4, \tag{62}$$

where

$$\begin{aligned}
\Theta_1 &= \frac{1}{2}\left(A - A^* - A^* \ln \frac{A}{A^*}\right)^2, \\
\Theta_2 &= \frac{1}{2}\left(F - F^* - F^* \ln \frac{F}{F^*}\right)^2, \\
\Theta_3 &= \frac{1}{2}\left(I - I^* - I^* \ln \frac{I}{I^*}\right)^2, \\
\Theta_4 &= \frac{1}{2}\left(S + A + P + F + I - S^* - P^* - A^* - F^* - I^*\right)^2.
\end{aligned} \tag{63}$$

The differential operator L for Θ_1 is:

$$\begin{aligned}
L\Theta_1 &= \left(1 - \frac{A^*}{A}\right)(dP - \delta AI + \theta F - m_3 A) + \frac{1}{2}\frac{A^*}{A^2}\left(\rho_1^2 A^2 I^2\right) \\
&= \left(A - A^*\right)\left(\frac{dP}{A} + \frac{\theta F}{A} - \delta I - m_3\right) + \frac{1}{2}\rho_1^2 A^* I^2 \\
&= \left(A - A^*\right)\left(\frac{dP(A^* - A)}{AA^*} + \frac{d(P - P^*)}{A^*} + \frac{\theta F(A^* - A)}{AA^*} + \frac{\theta(F - F^*)}{A^*}\right. \\
&\quad \left. + \delta\left(I^* - I\right)\right) + \frac{1}{2}\rho_1^2 A^* I^2 \\
&\le \frac{d(P - P^*)(A - A^*)}{A^*} + \frac{\theta(F - F^*)(A - A^*)}{A^*} + \delta\left(I^* - I\right)\left(A - A^*\right) \\
&\quad + \frac{1}{2}\rho_1^2 A^* I^2.
\end{aligned} \tag{64}$$

By computation, it can be obtained as:

$$\begin{aligned}
L\Theta_1 &\le \frac{d(P - P^*)(A - A^*)}{A^*} + \frac{\theta(F - F^*)(A - A^*)}{A^*} + \delta\left(I^* - I\right)\left(A - A^*\right) \\
&\quad + \frac{1}{2}\rho_1^2 A^*\left(I - I^* + I^*\right)^2 \\
&\le \frac{d(P - P^*)(A - A^*)}{A^*} + \frac{\theta(F - F^*)(A - A^*)}{A^*} + \delta\left(I^* - I\right)\left(A - A^*\right) \\
&\quad + \frac{1}{2}\rho_1^2 A^*\left(I - I^*\right)^2 + \frac{1}{2}\rho_1^2 A^*\left(I^*\right)^2.
\end{aligned} \tag{65}$$

Similarly, the differential operator L for Θ_2 can be computed as:

$$\begin{aligned}
L\Theta_2 &= \left(1 - \frac{F^*}{F}\right)(\eta P - \sigma FI + \varphi A - m_4 F) + \frac{1}{2}\frac{F^*}{F^2}\left(\rho_2^2 F^2 I^2\right) \\
&= \left(F - F^*\right)\left(\frac{\eta P}{F} - \sigma I + \frac{\varphi A}{F} - m_4\right) + \frac{1}{2}F^* \rho_2^2 I^2 \\
&= \left(F - F^*\right)\left(\frac{\eta P(F^* - F)}{FF^*} + \frac{\eta(P - P^*)}{F^*} + \frac{\varphi A(F^* - F)}{FF^*} + \frac{\varphi(A - A^*)}{F^*}\right.
\end{aligned} \tag{66}$$

$$
\begin{aligned}
&+\sigma\left(I^*-I\right)\Big)+\frac{1}{2}\rho_2^2F^*\left(I-I^*+I^*\right)^2\\
\leq&\frac{\eta(P-P^*)(F-F^*)}{F^*}+\frac{\varphi(A-A^*)(F-F^*)}{F^*}+\sigma\left(I^*-I\right)\left(F-F^*\right)\\
&+\frac{1}{2}\rho_2^2F^*\left(I-I^*\right)^2+\frac{1}{2}\rho_2^2F^*\left(I^*\right)^2.
\end{aligned}
$$

Next, the differential operator L for Θ_3 is calculated as:

$$
\begin{aligned}
L\Theta_3=&\left(1-\frac{I^*}{I}\right)(\delta AI+\sigma FI+\beta SI-m_5I)+\frac{1}{2}\frac{I^*}{I^2}\left(\rho_1^2A^2I^2+\rho_2^2F^2I^2\right)\\
=&\left(I-I^*\right)(\delta A+\sigma F+\beta S-m_5)+\frac{1}{2}I^*\left(\rho_1^2A^2+\rho_2^2F^2\right)\\
=&\delta\left(I-I^*\right)\left(A-A^*\right)+\sigma\left(I-I^*\right)\left(F-F^*\right)+\beta\left(I-I^*\right)\left(S-S^*\right)\\
&+\frac{1}{2}\rho_1^2I^*\left(A-A^*+A^*\right)^2+\frac{1}{2}\rho_2^2\left(F-F^*+F^*\right)^2\\
\leq&\delta\left(I-I^*\right)\left(A-A^*\right)+\sigma\left(I-I^*\right)\left(F-F^*\right)+\beta\left(I-I^*\right)\left(S-S^*\right)\\
&+\frac{1}{2}\rho_1^2I^*\left(A-A^*\right)^2+\frac{1}{2}\rho_1^2I^*\left(A^*\right)^2+\frac{1}{2}\rho_2^2I^*\left(F-F^*\right)^2+\frac{1}{2}\rho_2^2I^*\left(F^*\right)^2.
\end{aligned}
\tag{67}
$$

Finally, the differential operator L for Θ_3 can be computed as:

$$
\begin{aligned}
L\Theta_4=&\left(S+P+A+F+I-S^*-P^*-A^*-F^*-I^*\right)\left(-\mu\left(S-S^*\right)\right.\\
&\left.-\mu\left(P-P^*\right)-\mu\left(A-A^*\right)-\mu\left(F-F^*\right)-(\mu+\varepsilon)\left(I-I^*\right)\right)\\
=&-\mu\left(S-S^*\right)^2-2\mu\left(P-P^*\right)\left(S-S^*\right)-2\mu\left(A-A^*\right)\left(S-S^*\right)\\
&-2\mu\left(F-F^*\right)\left(S-S^*\right)-2(\mu+\varepsilon)\left(I-I^*\right)\left(S-S^*\right)-\mu\left(P-P^*\right)^2\\
&-2\mu\left(A-A^*\right)\left(P-P^*\right)-2\mu\left(F-F^*\right)\left(P-P^*\right)-2(\mu+\varepsilon)\left(I-I^*\right)\left(P-P^*\right)\\
&-\mu\left(A-A^*\right)^2-2\mu\left(F-F^*\right)\left(A-A^*\right)-2(\mu+\varepsilon)\left(I-I^*\right)\left(A-A^*\right)\\
&-\mu\left(F-F^*\right)^2-2(\mu+\varepsilon)\left(I-I^*\right)\left(F-F^*\right)-(\mu+\varepsilon)\left(I-I^*\right)^2.
\end{aligned}
\tag{68}
$$

Combining the above equations, there is:

$$
\begin{aligned}
\Theta(S,P,A,F,I,R)\leq&\frac{1}{2}\rho_1^2A^*\left(I-I^*\right)^2+\frac{1}{2}\rho_1^2A^*\left(I^*\right)^2+\frac{1}{2}\rho_2^2F^*\left(I-I^*\right)^2+\frac{1}{2}\rho_2^2F^*\left(I^*\right)\\
&+\frac{1}{2}\rho_1^2I^*\left(A-A^*\right)^2+\frac{1}{2}\rho_1^2I^*\left(A^*\right)^2+\frac{1}{2}\rho_2^2I^*\left(F-F^*\right)^2+\frac{1}{2}\rho_2^2I^*\left(F^*\right)^2\\
&-\mu\left(S-S^*\right)^2-\mu\left(P-P^*\right)^2-\mu\left(A-A^*\right)^2-(\mu+\varepsilon)\left(I-I^*\right)^2\\
=&-\mu\left(S-S^*\right)^2-\mu\left(P-P^*\right)^2-\left(\mu-\frac{1}{2}\rho_1^2I^*\right)\left(A-A^*\right)^2\\
&-\left(\mu-\frac{1}{2}\rho_2^2I^*\right)\left(F-F^*\right)^2-\left(\mu+\varepsilon-\frac{1}{2}\rho_1^2A^*-\frac{1}{2}\rho_2^2F^*\right)\left(I-I^*\right)^2\\
&+\frac{1}{2}\rho_1^2A^*\left(I^*\right)^2+\frac{1}{2}\rho_2^2F^*\left(I^*\right)^2+\frac{1}{2}\rho_1^2I^*\left(A^*\right)^2+\frac{1}{2}\rho_2^2I^*\left(F^*\right)^2.
\end{aligned}
\tag{69}
$$

According to the equation (59), the ellipsoid

$$-\xi_1(S-S^*)^2-\xi_2(P-P^*)^2-\xi_3(A-A^*)^2-\xi_4(F-F^*)^2-\xi_5(I-I^*)^2+M=0 \tag{70}$$

lies entirely in R_+^5, and any region containing this ellipsoid is denoted as O, and $\overline{O}\in R_+^5$, where $\overline{O}$ is the closure of O. It can be deduced that $L\Theta(S,P,A,F,I,R)<0$ in $(S,P,A,F,I)\in R_+^5$. It is easily shown that the diffusion matrix of the system forms a uniform ellipsoid over O [41]. Based on the above analysis, obviously, the random system (61) has a stationary distribution π and is ergodic.

Specifically, there exists:

$$\begin{aligned}\lim_{t\to\infty}\frac{1}{t}E\int_0^t\big[&\xi_1\big(S(v)-S^*\big)^2+\xi_2\big(P(v)-P^*\big)^2+\xi_3\big(A(v)-A^*\big)^2+\xi_4\big(F(v)-F^*\big)^2\\&+\xi_5\big(I(v)-I^*\big)^2\big]dv\le M.\end{aligned} \tag{71}$$

□

Theorem 9 *In system* (46)*, given* $(S(t),P(t),A(t),F(t),I(t),R(t))\in\mathbb{R}_+^6$ *as a solution, for any initial condition* $(S^0,P^0,A^0,F^0,I^0,R^0)\in\mathbb{R}_+^6$*, if* $G(\rho_1^2,\rho_2^2)=\frac{\delta^2}{2\rho_1^2}+\frac{\sigma^2}{2\rho_2^2}+\frac{\beta b}{\mu}-m_5<0$*, then* $\limsup_{t\to\infty}\frac{\ln I(t)}{t}<0$*,* $I(t)$ *tends to* 0.

Proof From equation (47), we can obtain that:

$$\begin{aligned}d\ln I(t)=&\left(\delta A(t)+\sigma F(t)-m_5+\beta S(t)-\frac{\rho_1^2A^2(t)}{2}-\frac{\rho_2^2F^2(t)}{2}\right)dt\\&+\rho_1A(t)dW_1(t)+\rho_2F(t)dW_2(t).\end{aligned} \tag{72}$$

Integrating both sides of the equation over t in the interval $[0,t]$, and dividing by t, then the deformation is:

$$\begin{aligned}\frac{\ln I(t)-\ln I(0)}{t}=&\frac{\int_0^t(\delta A(h)+\sigma F(h)+\beta S(h)-m_5-\frac{\rho_1^2A^2(h)}{2}-\frac{\rho_2^2F^2(h)}{2})dh}{t}\\&+\frac{\int_0^t\rho_1A(h)dW_1(h)}{t}+\frac{\int_0^t\rho_2F(h)dW_2(h)}{t},\end{aligned} \tag{73}$$

then

$$\begin{aligned}\frac{\ln I(t)}{t}=&\frac{\int_0^t(\delta A(h)+\sigma F(h)+\beta S(h)-m_5-\frac{\rho_1^2A^2(h)}{2}-\frac{\rho_2^2F^2(h)}{2})dh}{t}\\&+\frac{\int_0^t\rho_1A(h)dW_1(h)}{t}+\frac{\int_0^t\rho_2F(h)dW_2(h)}{t}+\frac{\ln I(0)}{t}\\\le&\frac{\int_0^t(-\frac{\rho_1^2}{2}(A(h)-\frac{\delta}{\rho_1^2})^2+\frac{\delta^2}{2\rho_1^2})dh}{t}+\frac{\int_0^t(-\frac{\rho_2^2}{2}(F(h)-\frac{\sigma}{\rho_2^2})^2)dh}{t}\\&+\frac{\sigma^2}{2\rho_2^2}+\frac{\beta b}{\mu}-m_5+\frac{\int_0^t\rho_1A(h)dW_1(h)}{t}+\frac{\int_0^t\rho_2F(h)dW_2(h)}{t}+\frac{\ln I(0)}{t}\\\le&\frac{\delta^2}{2\rho_1^2}+\frac{\sigma^2}{2\rho_2^2}+\frac{\beta b}{\mu}-m_5+\frac{\int_0^t\rho_1A(h)dW_1(h)}{t}+\frac{\int_0^t\rho_2F(h)dW_2(h)}{t}+\frac{\ln I(0)}{t},\end{aligned} \tag{74}$$

where $\int_0^t\rho_1A(h)dW_1(h)$ and $\int_0^t\rho_2F(h)dW_2(h)$ are continuous local martingales.

Let $Q_1(t) = \int_0^t \rho_1 A(h)dW_1(h)$ and $Q_2(t) = \int_0^t \rho_2 F(h)dW_2(h)$ with $Q_1(0) = 0$ and $Q_2(0) = 0$, where the quadratic variations can be represented as:

$$\langle Q_1(t)\rangle = \rho_1^2 \int_0^t A^2(h)dh, \tag{75}$$

$$\langle Q_2(t)\rangle = \rho_2^2 \int_0^t F^2(h)dh. \tag{76}$$

According to the positive invariant set (6), there exists $\limsup_{t\to\infty} \frac{\langle Q_i(t)\rangle}{t} \le \frac{\rho_i^2 b^2}{\mu^2} < \infty$, and $\lim_{t\to\infty} \frac{Q_i(t)}{t} = 0$ can be obtained by the strong law of number. Then, we take the upper limit of equation (74), to obtain:

$$\limsup_{t\to\infty} \frac{\ln I(t)}{t} \le \frac{\delta^2}{2\rho_1^2} + \frac{\sigma^2}{2\rho_2^2} + \frac{\beta b}{\mu} - m_5. \tag{77}$$

To eradicate the disease, it suffices to satisfy $\limsup_{t\to\infty} \frac{\ln I(t)}{t} < 0$. Setting $G(\rho_1^2, \rho_2^2) = \frac{\delta^2}{2\rho_1^2} + \frac{\sigma^2}{2\rho_2^2} + \frac{\beta b}{\mu} - m_5$, it can be seen that $G(\rho_1^2, \rho_2^2)$ is monotonically declining with respect to ρ_1^2 and ρ_2^2. Therefore, as long as ρ_1^2 and ρ_2^2 are sufficiently large such that the disease will ultimately disappear, simultaneously, there exists $G(\rho_1^2, \rho_2^2) < 0$. □

The analysis of the stochastic model demonstrates that disease can naturally die out under certain conditions, particularly when the intensity of random perturbations is sufficiently large. Biologically, this implies that the randomness in policies, such as intermittent lockdown or fluctuating vaccination rate, can to some extent weaken the long-term transmission potential of the disease.

7 Numerical simulations

Combined with the findings of this study, the Runge–Kutta algorithm was implemented to perform numerical simulations. As the parameter ranges were not provided in previous research, this paper establishes them based on R_0 and stability conditions to ensure model accuracy. The outcome of these simulations supports the validity of the theories presented.

For the verification of the local asymptotic stability of E_0 in Theorem 1. Let $b = 0.00752$, $\alpha = 0.3$, $\varphi = 0.2$, $\theta = 0.2$, $\eta = 0.3$, $\omega = 0.2$, $d = 0.3$, $\beta = 0.4$, $\delta = 0.3$, $\sigma = 0.5$, $\varepsilon = 0.6$, $\phi = 0.0001$, $\mu = 0.0074$. Through calculations, $R_{01} = 0.6612$, $R_0 = R_{02} = 0.96432 < 1$ and the equilibrium point $E_0 = (0.0323, 0.0120, 0.4860, 0.4860, 0, 0)$ can be concluded. The local asymptotic stability of the model (2) at E_0 is confirmed by Fig. 2, which indicates that the infectious disease will eventually be eradicated over time.

To verify the local asymptotic stability of E^* in Theorem 2, let $b = 0.00752$, $\alpha = 0.3$, $\varphi = 0.2$, $\theta = 0.2$, $\eta = 0.3$, $\omega = 0.3$, $d = 0.3$, $\beta = 0.4$, $\delta = 0.3$, $\sigma = 0.5$, $\varepsilon = 0.1270$, $\phi = 0.0001$, $\mu = 0.0074$. The calculations yield $R_{02} = 0.96432$, $R_0 = R_{01} = 2.9866 > 1$ and $E^* = (0.0303, 0.0113, 0.1546, 0.1519, 0.0368, 0.6308)$. Figure 3 confirms the local asymptotic stability of E^* in model (2) and indicates that the infectious disease will eventually converge to the positive equilibrium point E^* as time progresses.

To reveal the influence of the optimal control pair $(\chi_1^*(t), \chi_2^*(t), d^*(t), \theta^*(t))$ on disease spread with the optimal control strategy, a group of parameters is randomly set: $b = 0.00752$, $\alpha = 0.3$, $\omega = 0.2$, $\eta = 0.3$, $\varphi = 0.2$, $\beta = 0.4$, $\delta = 0.3$, $\sigma = 0.5$, $\varepsilon = 0.6$, $\phi = 0.0001$, $\mu = 0.0074$, and let $\chi_1 = \chi_1^*(t)$, $\chi_2 = \chi_2^*(t)$, $d = d^*(t)$, $\theta = \theta^*(t)$. Meanwhile, different control

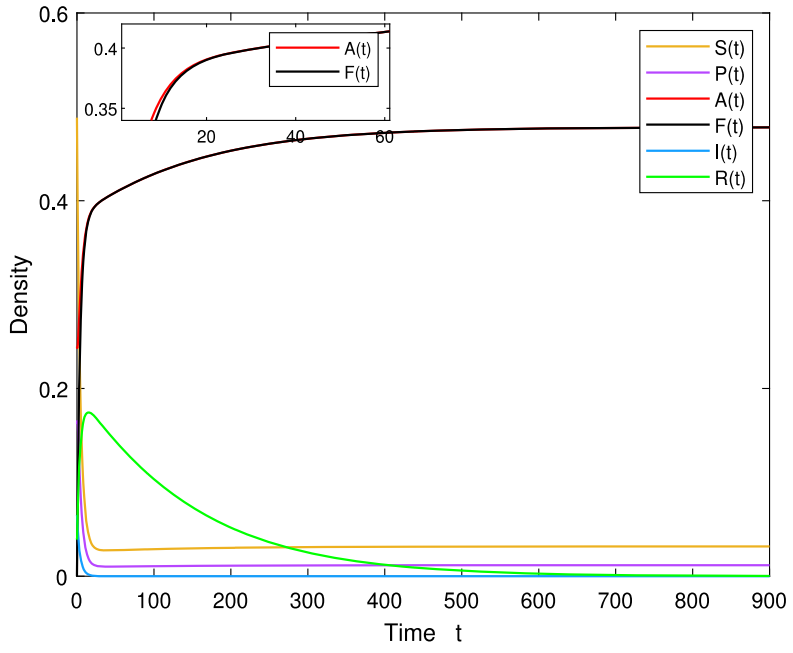

Figure 2 Stability of E_0 for the model (2) when $R_0 < 1$

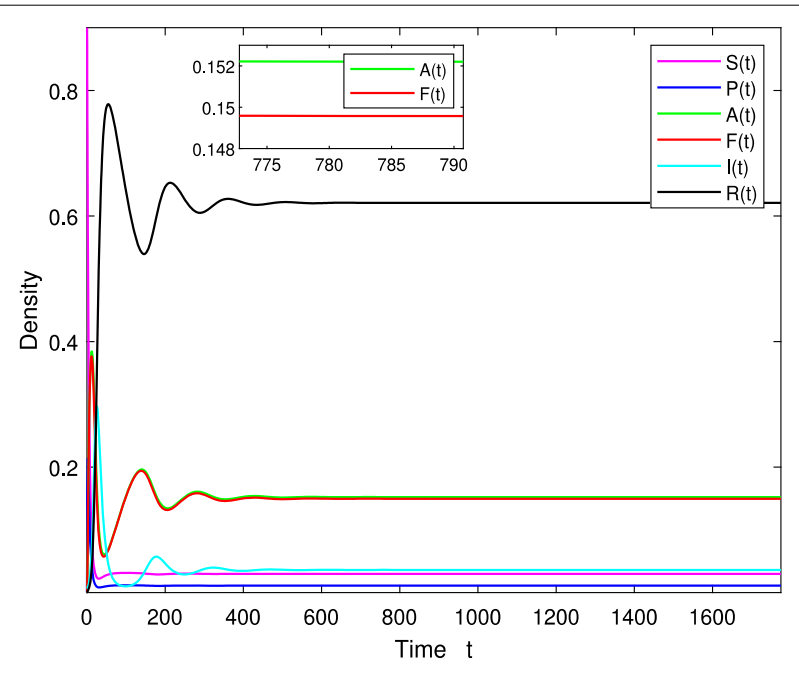

Figure 3 Stability of E^* for system (2) with $R_0 > 1$ and $\beta m_2 m_5(\sigma m_3 + \delta m_4) + \delta\sigma(m_5(m_1 m_2 - \omega\alpha)) > \delta\sigma b\beta m_2$

strategies are applied: "optimal control", "middle control measure", and "constant control measure". The images of different control strategies can be obtained. Figure 4 shows the variation of the population of $A(t)$ and $I(t)$ with time t under different control strategies. In Fig. 4(a), $A(t)$ under the optimal control strategy shows a decreasing trend over time until it stabilizes, while $A(t)$ under the constant control strategy and middle control strategy

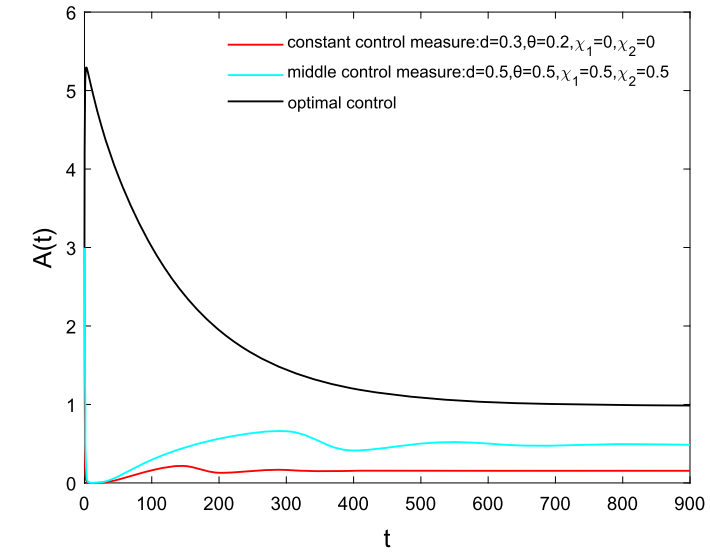

(a)

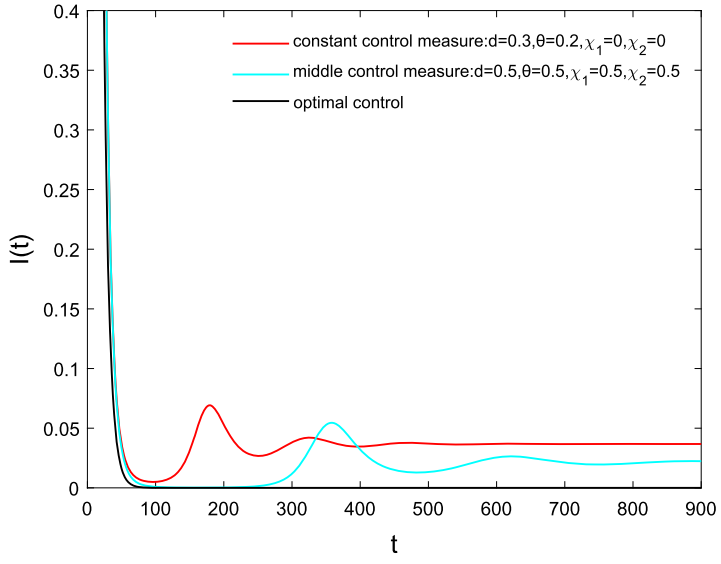

(b)

Figure 4 The fluctuations of $A(t)$ and $I(t)$ over time when employing various control strategies

requires some fluctuations over time before reaching a stable state. In Fig. 4(b), $I(t)$ under the optimal control strategy can reach a stable state in a very short time, and the number of people infected that reach the stable state under the middle control strategy is fewer than under the constant control strategy. However, under the middle control strategy, it takes longer for $I(t)$ to reach stability. According to Fig. 4, it is clear that "optimal control" is preferable to "medium control measure", while "constant control measure" is less desirable. This suggests that, in any case, the optimal control strategy is effective in controlling infectious disease and optimizing the number of infected individuals. However, it is im-

portant to note that optimal control requires multiple control measures to suppress the spread of infection through active prevention education and community encouragement

Next, Verification of the infectious disease eradication condition in the stochastic model (46). First, let $\rho_1 = 0.05$, $\rho_2 = 0.025$. Figure 5 presents the time series and frequencies of $S(t)$, $A(t)$, $F(t)$, and $I(t)$. According to Theorem 8, it is known that the disease will persist and there is a stationary distribution. Observing from Fig. 5, despite the continuous fluctuations in the count of susceptible, alert, fragile, and infected individuals over time t, the probabilities they follow are stable. Next, to observe the spread of infectious disease under deterministic and random systems, consider comparing the deterministic system with the random system with different perturbation intensities. For $\rho_1 = 0.05$, $\rho_2 = 0.025$, the changes of $S(t)$, $A(t)$, $F(t)$, and $I(t)$ in the deterministic and stochastic models are shown in Fig. 6. The quantities of individuals in the stochastic model fluctuate from the deterministic model, but over a smaller range. When the perturbations rise so that $\rho_1 = 0.085$, $\rho_2 = 0.05$, from Fig. 7, one can observe that the individuals in the stochastic model fluctuate more, but still oscillate around the equilibrium of the deterministic model and remain stationary overall.

The more pronounced fluctuations observed in Fig. 7 are a result of the increased perturbation intensity incorporated into the model. These variations illustrate the influence of random factors on the system, particularly in real-world situations such as localized outbreaks or in small populations. During the initial phases of an outbreak, for instance, patient numbers may fluctuate significantly due to random influences like changes in contact rates, despite the overall trend eventually stabilizing toward the equilibrium point. This demonstrates how stochastic factors, such as variability in contact rates or environmental shifts, can cause notable short-term deviations from equilibrium, even when the long-term trend remains steady.

Let $b = 0.0074$, $\alpha = 0.3$, $\varphi = 0.2$, $\theta = 0.2$, $\omega = 0.2$, $d = 0.3$, $\eta = 0.3$, $\beta = 0.2$, $\delta = 0.15$, $\sigma = 0.3$, $\varepsilon = 0.85$, $\phi = 0.25$, $\mu = 0.3$, $\rho_1 = 0.25$, $\rho_2 = 0.25$, which satisfy Theorem 9. Figure 8 displays the time series of $S(t)$, $A(t)$, $F(t)$, and $I(t)$. When the perturbation intensities are large enough, the populations of susceptible, alert, and vulnerable individuals can instantly increase and reach a steady state. Simultaneously, the number of infected individuals can instantly decrease to 0, which means that at sufficiently high perturbation intensities, the infection dies out instantly. Therefore, over time, rapid extinction of the infectious disease can be accomplished by adding sufficient perturbations.

8 Sensitivity analysis

To explore the significance of effective contact rates in the process of virus transmission, this paper performs a sensitivity analysis on R_0 of the viral infection.

The partial derivatives of R_{01} in terms of the contact infection coefficients β, δ, and σ can be expressed, respectively, as follows:

$$\frac{\partial R_{01}}{\partial \beta} = \frac{b\beta m_2(m_3m_4 - \theta\varphi)}{\delta\alpha b(dm_4 + \theta\eta) + \sigma\alpha b(d\varphi + \eta m_3) + b\beta m_2(m_3m_4 - \theta\varphi)} > 0, \tag{78}$$

$$\frac{\partial R_{01}}{\partial \delta} = \frac{\delta\alpha b(dm_4 + \theta\eta)}{\delta\alpha b(dm_4 + \theta\eta) + \sigma\alpha b(d\varphi + \eta m_3) + b\beta m_2(m_3m_4 - \theta\varphi)} > 0, \tag{79}$$

$$\frac{\partial R_{01}}{\partial \sigma} = \frac{\sigma\alpha b(d\varphi + \eta m_3)}{\delta\alpha b(dm_4 + \theta\eta) + \sigma\alpha b(d\varphi + \eta m_3) + b\beta m_2(m_3m_4 - \theta\varphi)} > 0. \tag{80}$$

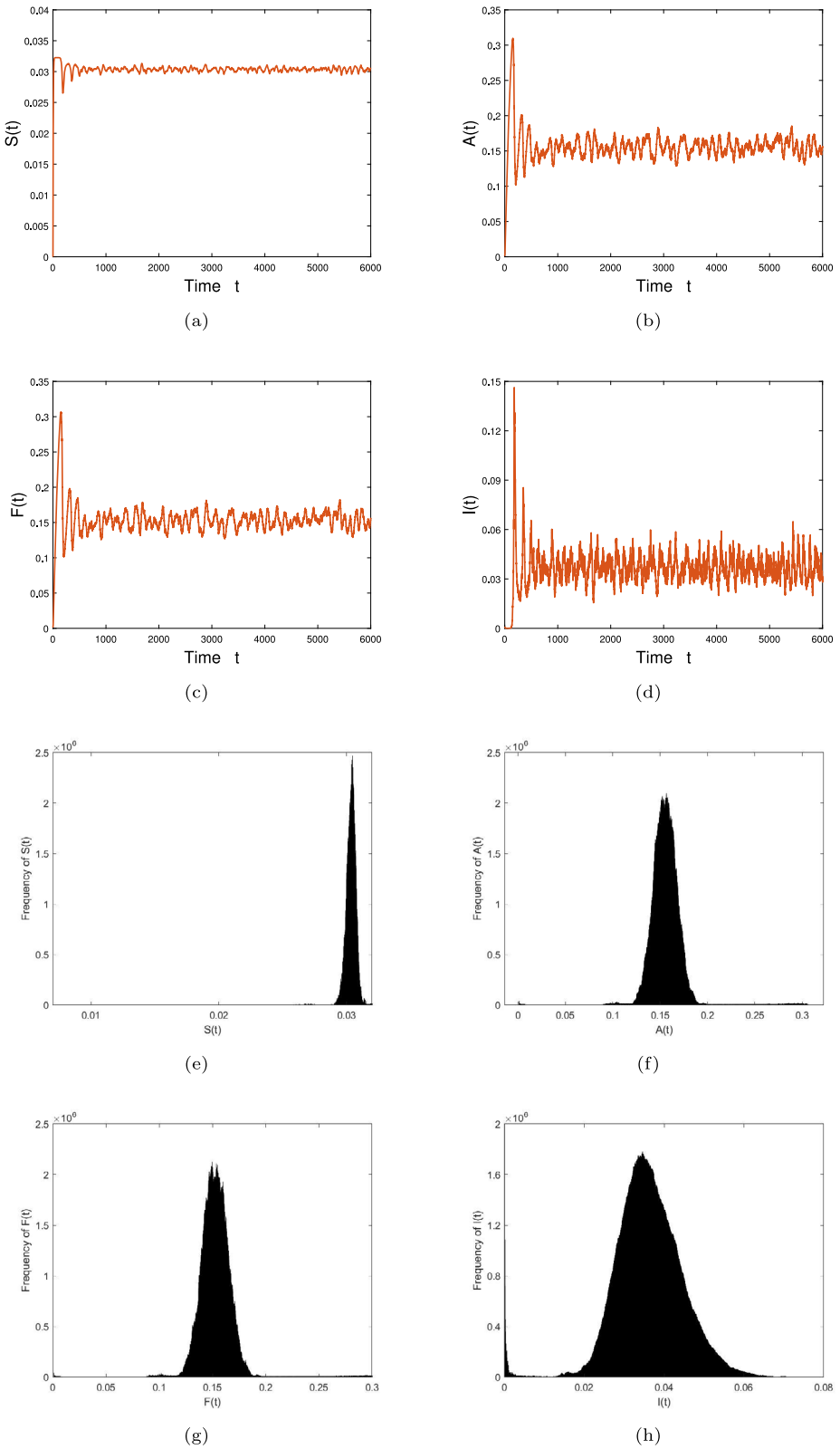

Figure 5 The time series and frequencies of $S(t)$, $A(t)$, $F(t)$, and $I(t)$ with $\rho_1 = 0.05$, $\rho_2 = 0.025$

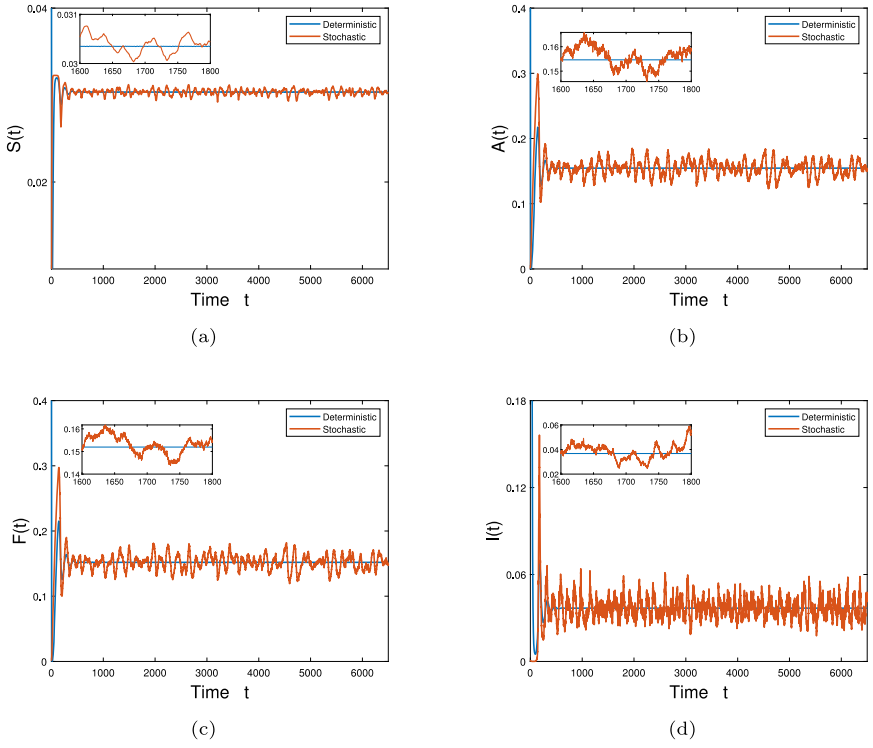

Figure 6 The deviations of $S(t)$, $A(t)$, $F(t)$, and $I(t)$ over time in both the deterministic and stochastic models, taking into account $\rho_1 = 0.05$ and $\rho_2 = 0.025$

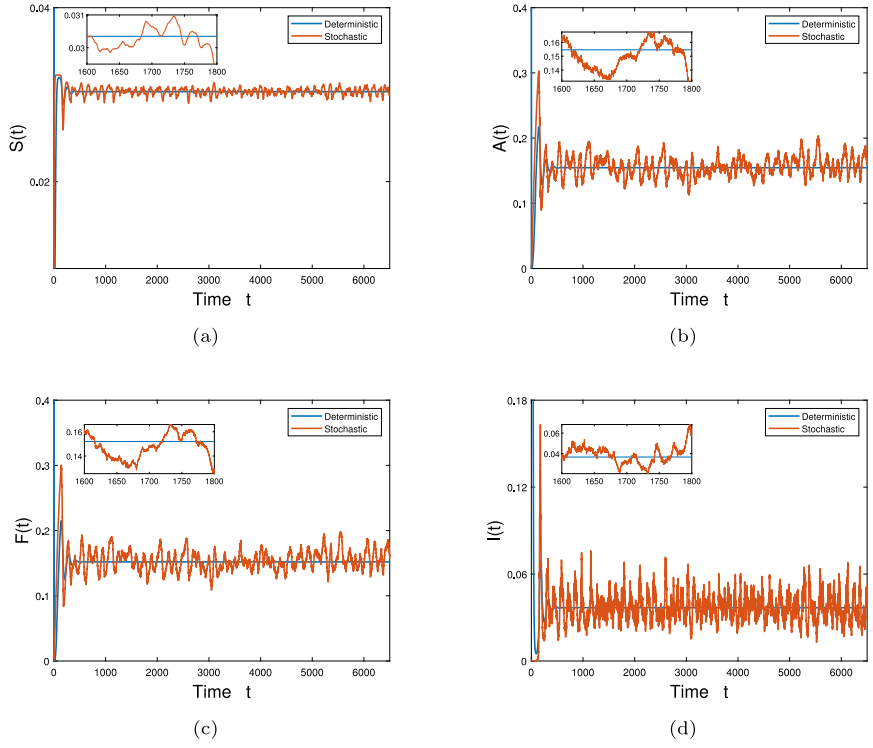

Figure 7 The disparities of $S(t)$, $A(t)$, $F(t)$, and $I(t)$ over time in both deterministic and stochastic models considering $\rho_1 = 0.085$ and $\rho_2 = 0.05$

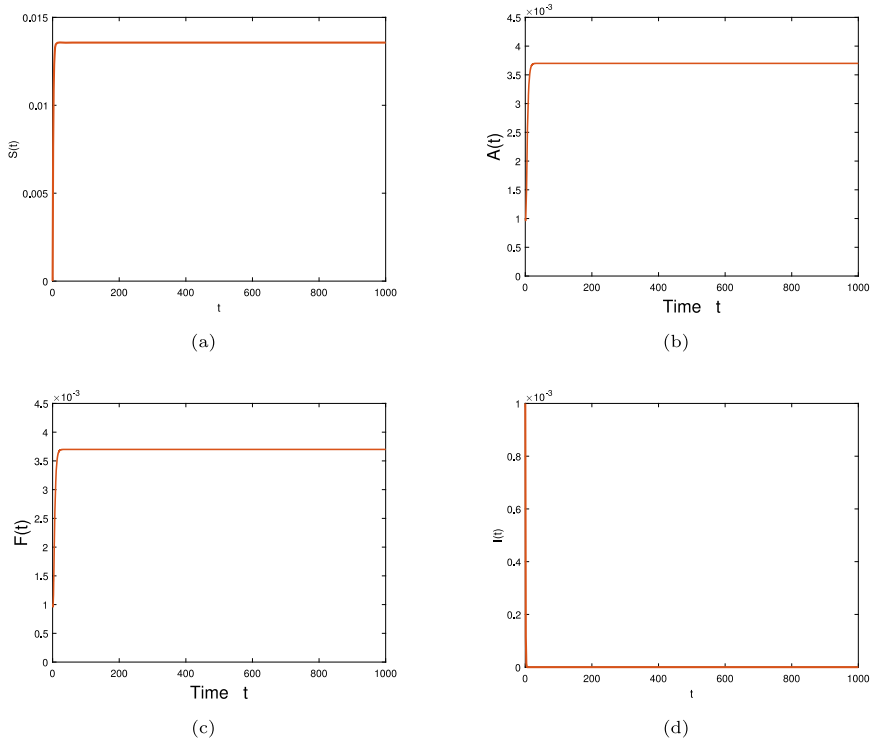

Figure 8 The temporal evolution of $S(t)$, $A(t)$, $F(t)$, and $I(t)$ with $\rho_1 = 0.25$ and $\rho_2 = 0.25$

It is clearly shown that parameters β, δ, and σ help to suppress the infection and transmission of the virus.

Figure 9 presents the sensitivity analysis of R_{01}. Specifically, Fig. 9(a) illustrates the sensitivity of R_{01} to the effective contact rates δ and β. It is evident that R_{01} remains unaffected by changes in the parameter β, whereas its value increases with the increment of the parameter δ. Similarly, Fig. 9(b) demonstrates the sensitivity of R_{01} to the effective contact rates σ and β. In this case as well, R_{01} does not exhibit any variation with respect to the parameter β, while its value rises with an increase in the parameter σ. Furthermore, Fig. 9(c) displays the sensitivity analysis of R_{01} to the effective contact rates σ and δ. Here, the value of R_{01} increases with the increment of both parameters, showing consistent growth magnitudes. Based on Fig. 9(a), if there exists $R_0 = R_{01}$, parameters δ and σ have a greater inhibitory effect on the virus than parameter β. Therefore, Spreading the virus can be effectively curbed by intervening the individual behavioral responses of pseudoinfected individuals.

R_{02} is independent of parameters β, δ, and σ, so the sensitivity analysis of R_{02} is not performed in this paper.

9 Conclusions

To explore the impact of behavioral responses of pseudoinfected individuals on virus transmission, this paper develops the SPAFIR epidemic model including "pseudoinfected individuals", "alert individuals", and "susceptible individuals", which can indicate the impact of pseudoinfected individuals' behavioral responses on infectious-disease transmission. Furthermore, the impact of random fluctuations in effective contact rates is consid-

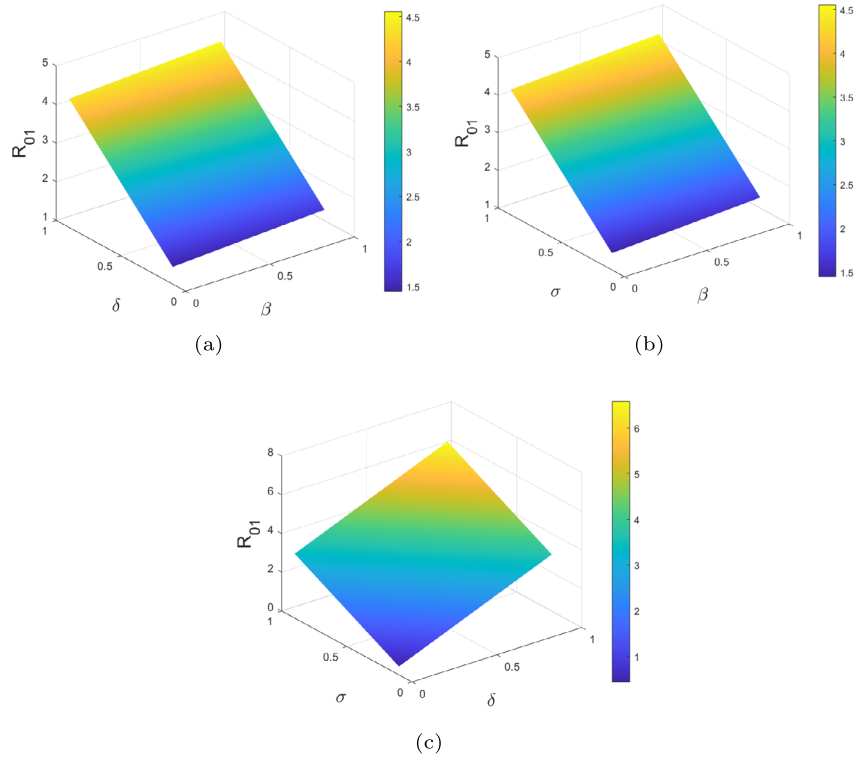

Figure 9 The sensitivity analysis of R_{01} to the effective contact rates δ, σ, and β

ered. Finally, to validate the results derived from the theoretical analysis and evaluate how the model responds to variations in the effective contact rates, numerical simulations are conducted.

In comparison to the classical SIR model, this paper explores in depth the impact of "pseudoinfection" and "individual behavior" on spreading the infectious disease, making the system more realistic in terms of the actual scenario of disease spread. Also, this paper incorporates the impact of pseudoinfection, enabling the model to better predict the trend of disease spread. Thus, the model proposed in this paper provides an accurate and practical tool for studying transmission mechanisms and formulating infectious disease control strategy. Through the research, the following results have been obtained: i) Positive individual behavioral responses can reduce infection spread. ii) Active prevention education and community encouragement can help prevent the infectious disease from spreading, but they cannot completely eliminate the infection. iii) Random fluctuations in effective contact rates can suppress infection spread, so taking full advantage of stochastic perturbations in the effective contact rate can achieve the inhibitory effect on disease spread.

Future investigations will prioritize three specific areas. Firstly, we will examine the transmission of multiple viruses within the social system. Secondly, we will investigate the effect of individuals falsely diagnosed with infection on the dissemination of different contagious illnesses during the same era within the societal framework. Lastly, future research will examine stochastic perturbations to enhance the effectiveness of contact rates

and explore the circumstances under which disease extinction occurs in the scenario of multiple viruses.

Acknowledgements
We sincerely thank the anonymous Editors and Reviewers for their earnest feedback.

Author contributions
XN: Conceptualization, methodology, and writing the original draft. YH: Methodology, reviewing, and editing. WY: Visualization and supervision. All authors read and approved the final manuscript.

Funding
This work was supported by the Social Science Planning Fund of Liaoning Province China (No. L22AGL015).

Data availability
This article has no associated data.

Declarations

Competing interests
The authors declare that they have no competing interests.

Author details
[1]School of Science, University of Science and Technology Liaoning, Qianshan Middle Road, Anshan, 114051, Liaoning, China. [2]School of General Education, Dalian Neusoft University of Information, Software Park Road, Dalian, 116023, China.

Received: 22 October 2024 Accepted: 14 January 2025 Published online: 24 January 2025

References

1. Mostafavi, E., Ghasemian, A., Abdinasir, A., et al.: Emerging and re-emerging infectious diseases in the who eastern Mediterranean region, 2001-2018. Int. J. Health Policy Manag. **11**(8), 1286–1300 (2022)
2. Kushner, H.I.: Epidemics and history: Disease, power, and imperialism. By Sheldon Watts (New Haven: Yale University Press, 1997. xvi plus 400pp.). J. Soc. Hist. **32**(4), 995–997 (1999)
3. Snowden, F.M.: Epidemics and Society: From the Black Death to the Present. Yale University Press, New Haven (2019)
4. Morse, S.S., Schluederberg, A.: Emerging viruses: the evolution of viruses and viral diseases. J. Infect. Dis. **162**(1), 1–7 (1990)
5. Weiss, R.A., McMichael, A.J.: Social and environmental risk factors in the emergence of infectious diseases. Nat. Med. **10**(12), S70–S76 (2004)
6. Ullah, S.: Impact of COVID-19 pandemic on financial markets: a global perspective. J. Knowl. Econ. **14**, 982–1003 (2022)
7. Shang, Y., Li, H., Zhang, R.: Effects of pandemic outbreak on economies: evidence from business history context. Front. Public Health **9**, 632043 (2021)
8. Sigala, M.: Tourism and COVID-19: impacts and implications for advancing and resetting industry and research. J. Bus. Res. **117**, 312–321 (2020)
9. Dolnicar, S., Zare, S.: COVID-19 and Airbnb – disrupting the disruptor. Ann. Tour. Res. **83**, 102961 (2020)
10. Li, Z., Zhang, S., Liu, X., et al.: Seeing the invisible hand: underlying effects of COVID-19 on tourists' behavioral patterns. J. Destination Mark. Manag. **18**, 100502 (2020)
11. Bernoulli, D.: Essai d'une nouvelle analyse de la mortalité causée par la petite vérole et des avantages de l'inoculation pour la prévenir. Académie Royale des Sciences, Paris (1760)
12. Kermack, W.O., McKendrick, A.G.: A contribution to the mathematical theory of epidemics. Proc. R. Soc. Lond. Ser. A **115**(772), 700–721 (1927). Containing papers of a mathematical and physical character
13. Bailey, N.: The Mathematical Theory of Infectious Diseases and Its Applications. Charles Griffin & Company Ltd, Glasgow (1957)
14. Hethcote, H.W.: The mathematics of infectious diseases. SIAM Rev. **42**(4), 599–653 (2000)
15. Pariyaporn, R.O., Chinviriyasit, W., Chinviriyasit, S.: The effect of incidence function in backward bifurcation for malaria model with temporary immunity. Math. Biosci. **265**, 47–64 (2015)
16. Wang, X., Liu, Z., Wang, L., et al.: An application of a novel geometric criterion to global-stability problems of a nonlinear SEIVS epidemic model. J. Appl. Math. Comput. **67**(1–2), 707–730 (2021)
17. Xu, R., Ma, Z.: Global stability of a SIR epidemic model with nonlinear incidence rate and time delay. Nonlinear Anal., Real World Appl. **10**(5), 3175–3189 (2009)
18. Li, L., Sun, G.Q., Jin, Z.: Bifurcation and chaos in an epidemic model with nonlinear incidence rates. Appl. Math. Comput. **216**(4), 1226–1234 (2010)
19. Feng, Y.X., Li, W.T., Ruan, S., et al.: Dynamics and asymptotic profiles of a nonlocal dispersal SIS epidemic model with bilinear incidence and Neumann boundary conditions. J. Differ. Equ. **335**, 294–346 (2022)
20. Wu, Y., Zou, X.: Asymptotic profiles of steady states for a diffusive SIS epidemic model with mass action infection mechanism. J. Differ. Equ. **261**(8), 4424–4447 (2016)
21. Wen, X., Ji, J., Li, B.: Asymptotic profiles of the endemic equilibrium to a diffusive SIS epidemic model with mass action infection mechanism. J. Math. Anal. Appl. **458**(1), 715–729 (2018)
22. Satorras, R.P., Vespignani, A.: Epidemic spreading in scale-free networks. Phys. Rev. Lett. **86**, 3200–3203 (2001)

23. Boccaletti, S., Latora, V., Moreno, Y., et al.: Complex networks: structure and dynamics. Phys. Rep. **424**(4), 175–308 (2006)
24. Boccaletti, S., Almendral, J., Guan, S., et al.: Explosive transitions in complex networks' structure and dynamics: percolation and synchronization. Phys. Rep. **660**, 1–94 (2016)
25. Belik, V., Geisel, T., Brockmann, D.: Natural human mobility patterns and spatial spread of infectious diseases. Phys. Rev. X **1**, 011001 (2011)
26. Ge, J., Kim, K.I., Lin, Z., et al.: A SIS reaction–diffusion–advection model in a low-risk and high-risk domain. J. Differ. Equ. **259**(10), 5486–5509 (2015)
27. Wang, B.G., Li, W.T., Wang, Z.C.: A reaction-diffusion SIS epidemic model in an almost periodic environment. Z. Angew. Math. Phys. **66**(6), 3085–3108 (2015)
28. Zaman, G., Kang, Y.H., Cho, G., et al.: Optimal strategy of vaccination & treatment in an SIR epidemic model. Math. Comput. Simul. **136**, 63–77 (2017)
29. Zhang, J., Ma, Z.: Global dynamics of an SEIR epidemic model with saturating contact rate. Math. Biosci. **185**(1), 15–32 (2003)
30. Laarabi, H., Abta, A., Hattaf, K.: Optimal control of a delayed SIRS epidemic model with vaccination and treatment. Acta Biotheor. **63**(2), 87–97 (2015)
31. May, R.M.: Stability and Complexity in Model Ecosystems. Princeton University Press, Princeton (1974)
32. Tornatore, E., Buccellato, S.M., Vetro, P.: Stability of a stochastic SIR system. Phys. A, Stat. Mech. Appl. **354**, 111–126 (2005)
33. Wei, F., Chen, F.: Stochastic permanence of an SIQS epidemic model with saturated incidence and independent random perturbations. Phys. A, Stat. Mech. Appl. **453**, 99–107 (2016)
34. Gray, A., Greenhalgh, D., Hu, L., et al.: A stochastic differential equation SIS epidemic model. SIAM J. Appl. Math. **71**(3), 876–902 (2011)
35. Kang, S., Hou, X., Hu, Y., et al.: Dynamic analysis and optimal control of a stochastic information spreading model considering super-spreader and implicit exposer with random parametric perturbations. Front. Phys. **11**, 1194804 (2023)
36. Fenichel, E.P., Chavez, C.C., Ceddia, M.G., et al.: Adaptive human behavior in epidemiological models. Proc. Natl. Acad. Sci. **108**(15), 6306–6311 (2011)
37. Sahneh, F.D., Chowdhury, F.N., Scoglio, C.M.: On the existence of a threshold for preventive behavioral responses to suppress epidemic spreading. Sci. Rep. **2**(1), 632 (2012)
38. Almalahi, M.A., Panchal, S.K., Shatanawi, W., et al.: Analytical study of transmission dynamics of 2019-nCoV pandemic via fractal fractional operator. Results Phys. **24**, 104045 (2021)
39. van den Driessche, P., Watmough, J.: Reproduction numbers and sub-threshold endemic equilibria for compartmental models of disease transmission. Math. Biosci. **180**(1), 29–48 (2002)
40. Lasalle, J.P.: The Stability of Dynamical Systems. SIAM, Philadelphia (1976)
41. Khasminskii, R.Z.: Stochastic Stability of Differential Equations. Springer, Berlin (1980)

Publisher's Note